energies

MDPI

Article

Single and Multi-Objective Optimal Power Flow Based on Hunger Games Search with Pareto Concept Optimization

Murtadha Al-Kaabi *, Virgil Dumbrava and Mircea Eremia

Department of Power Systems, Faculty of Energy, University Politehnica of Bucharest, 060029 Bucharest, Romania
* Correspondence: mmsk.1986s@gmail.com; Tel.: +40-964-7500580065

Abstract: In this study, a new meta-heuristic optimization method inspired by the behavioral choices of animals and hunger-driven activities, called hunger games search (HGS), is suggested to solve and formulate the single- and multi-objective optimal power flow problem in power systems. The main aim of this study is to optimize the objective functions, which are total fuel cost of generator, active power losses in transmission lines, total emission issued by fossil-fueled thermal units, voltage deviation at PQ bus, and voltage stability index. The proposed HGS approach is optimal and easy, avoids stagnation in local optima, and can solve multi-constrained objectives. Various single-and multi-objective (conflicting) functions were proposed simultaneously to solve OPF problems. The proposed algorithm (HGS) was developed to solve the multi-objective function, called the multi-objective hunger game search (MOHGS), by incorporating the proposed optimization (HGS) with Pareto optimization. The fuzzy membership theory is the function responsible to extract the best compromise solution from non-dominated solutions. The crowding distance is the strategies carried out to determine and ordering the Pareto non-dominated set. Two standard tests (IEEE 30 bus and IEEE 57 bus systems) are the power systems that were applied to investigate the performance of the proposed approaches (HGS and MOHGS) for solving single and multiple objective functions with 25 studied cases using MATLAB software. The numerical results obtained by the proposed approaches (HGS and MOHGS) were compared to other optimization algorithms in the literature. The numerical results confirmed the efficiency and superiority of the proposed approaches by achieving an optimal solution and giving the faster convergence characteristics in single objective functions and extracting the best compromise solution and well-distributed Pareto front solutions in multi-objective functions.

Keywords: multi-objective optimal power flow (MOOPF); hunger games search (HGS); multi-objective hunger games search (MOHGS); Pareto concept; fuzzy set theory; fuel cost; active power losses; emission; voltage deviation; voltage stability index

check for updates

Citation: Al-Kaabi, M.; Dumbrava, V.; Eremia, M. Single and Multi-Objective Optimal Power Flow Based on Hunger Games Search with Pareto Concept Optimization. *Energies* **2022**, *15*, 8328. https://doi.org/10.3390/en15228328

Academic Editors: Yuan Liao and Ke Xu

Received: 17 October 2022
Accepted: 2 November 2022
Published: 8 November 2022

Publisher's Note: MDPI stays neutral with regard to jurisdictional claims in published maps and institutional affiliations.

Copyright: © 2022 by the authors. Licensee MDPI, Basel, Switzerland. This article is an open access article distributed under the terms and conditions of the Creative Commons Attribution (CC BY) license (https://creativecommons.org/licenses/by/4.0/).

1. Introduction

Power flow is one of the most important tools used to analyze and operate the power system by finding out active power losses in transmission lines and reactive power injection on lines and calculating the voltage at different buses. Optimal power flow (OPF) is a non-convex, nonlinear, and large-scale problem. The main aim of using OPF in power systems is to obtain the optimal objective functions by setting the control variables. These control variables involve real power output of generation units except the slack bus, the voltages magnitude at PV bus, regulating tap setting at transformers, and the source VAR compensator connected to transmission lines with satisfying the equality and inequality constraints. The objective functions that will be optimized are the total fuel cost of generation units, active power losses in transmission lines, total emission, voltage deviation, and the voltage stability index of system. The first presentation of the OPF problem formulation was presented by Dommel and Tinney 1968 [1].

Traditional and metaheuristic optimization methods are the types used to solve OPF problems in the power system. Linear programming, Newton methods, gradient based method, quadratic programming, and dynamic programming are the traditional methods that were proposed to solve OPF problems [2]. To overcome these weaknesses, many metaheuristic optimization methods were developed to solve OPF problems, such as differential evolution (DE) [3], genetic algorithm (GA) [4], modified artificial bee colony (MABC) [5], improved differential evolution (IDE) [6,7], adaptive constraint differential evolution (ACDE) [8], enhanced adaptive differential evolution with self-adaptive (EJADE-SP) [9], crisscross search based grey wolf optimizer (GS-GWO) [10], Harris hawks optimization [11], and fruit fly optimization (FFO) [12]. The previous metaheuristic optimization methods were applied to single-objective OPF problems.

Recently, multi-objective OPF problems (MOOPF) are solved by several optimization methods. These problems are described as nonlinear and large-scale. For example, improved differential evolution algorithm (IDEA) have been developed to solve multi-objective functions, called the multi-objective improved differential evolution algorithm (MOIDEA) [13]. The multi-objective slime mould algorithm (MOSMA) was proposed as a new optimization method to solve multi-objective optimal power flow (MOOPF) problems [14]. The multi-objective backtracking search algorithm (MOBSA) was suggested as a new multi-objective approach to solve and formulate MOOPF problems on power systems [15]. The multi-objective evolutionary algorithm (MOEA) was proposed as novel hybrid decomposition and local dominance to solve MOOPF problems with conflicting objectives [16]. The author in Ref. [17] suggested a new multi-objective method, called the multi-objective search group algorithm (MOSGA), which efficiently solves MOOPF problems in power systems.

In this work, the hunger games search algorithm was proposed to solve single objective OPF problems. In addition, the proposed algorithm HGS was developed to solve multi-objective optimal power flow (MOOPF) problems, namely, the multi-objective hunger games search (MOHGS). The proposed approach integrates the Pareto concept with the fuzzy membership approach to determine the nondominated solutions and extract the best compromise solution, respectively. The main aim of this approach is to optimize the objective function by satisfying the equality and inequality constraints. The objective functions that are minimized are total fuel cost, active power losses on transmission lines, total emission, voltage deviation at PQ busses, and the voltage stability index of whole system. In a multi-objective function. these objective functions that will be optimized may be conflicting simultaneously, which means when the first objective function is minimized, the second objective function will be maximized and vice versa. Therefore, the main goal in using the multi-objective optimal power flow (MOOPF) is to find out the compromise solution among multiple objective functions.

The hunger games search (HGS) is a stochastic optimization algorithm inspired by the behavior of social animal cooperation, which is proportional to their level of hunger, by Y. Yang et al. in 2021 [18]. The HGS is characterized by high convergence speed, powerful local exploitation, and global exploration. The main contributions of this paper can be summarized as follows:

- The hunger games search (HGS) and the developed approach, multi-objective hunger game search (MOOPF), are proposed to solve for single-and multi-objective optimal power flow (MOOPF) in power systems. Pareto concept (PC), fuzzy membership function (FMF), and crowding distance (CD) are the approaches used to find out non-dominated Pareto fronts (NDPF), extract the best compromise solution (BCS), and rank and reduce the Pareto repository, respectively.
- The IEEE 30-bus and IEEE 57-bus tests are the power systems applied to 25 studied cases by using single and multiple (Bi, Tri, Quad, and Quinta) objective functions. The numerical results obtained by the proposed approaches (HGS and MOHGS) will be compared with known optimization methods in the literature.

The rest of the paper will be arranged as follows: Section 2 introduces the formulation of OPF problems. Section 3 is focused on single- and multi-objective OPF frameworks. The simulation results of proposed approaches (HGS and MOHGS) are presented in Section 4. Finally, this paper will be finished with the conclusion.

2. The Formulation of the OPF Problem

The main aim of applied single- and multi-objective OPF in power systems is to optimize the objective functions of single and multiple objectives (Bi, Tri, Quad, and Quinta) through setting optimal control variables (active power output of generators except for active power output of slack bus, voltage magnitude of PV bus, Source VAR compensator, and tap setting regulating of transformers) with satisfying equality and inequality constraints, simultaneously. The mathematical model can be formulated as follows:

$$\begin{aligned} &\text{Optimize} && f(x,u) = f_1(x,u), f_2(x,u), \ldots, f_{N_{obj}}(x,u) \\ &\text{subjected to} && g(x,u) = 0 \\ & && h(x,u) \leq 0 \end{aligned} \tag{1}$$

where $f\ (x,\ u)$, $g(x,\ u)$, and $h(x,\ u)$ represent the objective function to be optimized, equality, and inequality constraints, respectively. x and u are the state and control variables, respectively.

2.1. The State and Variables

The mathematical expression of the state variable x is:

$$x = \left[P_{G_1}, |V_{L_1}|, \cdots, \left|V_{L_{N_{PQ}}}\right|, Q_{G_1}, \cdots, Q_{G_{N_{PV}}}, S_{l_1}, \cdots, S_{l_{N_l}}\right] \tag{2}$$

where P_{G1} is the active power at slack bus; V_L is the voltage magnitude at load bus (PQ buses); Q_G is the reactive power at PV bus; and S_l is the transmission line loading; N_{PV}, N_{PQ}, and N_l denote numbers of generators, load buses, transmission lines, respectively. The mathematical expression of the state variable u is:

$$u = \left[P_{G_2}, \cdots, P_{G_{N_G}}, |V_{G_1}|, \cdots, \left|V_{G_{N_G}}\right|, T_1, \cdots, T_{N_T}, Q_{C_1}, \cdots, Q_{C_{N_C}}\right] \tag{3}$$

where P_G is the active power at the PV bus except the slack bus. V_G is the voltage magnitude at PV buses. T denotes the tap settings regulating transformers. Q_c is the source VAR compensator. N_G, N_T, and N_C are the numbers of generators, source VAR (shunt) compensators, and regulating transformers, respectively.

2.2. Objective Constraints

The constraints of OPF can be divided into equality and inequality constraints. The equality constraints represent the physical structure (the power balance equations) of the whole system.

$$\begin{aligned} &P_{Gi} - P_{Di} - |V_i| \sum_{j=1}^{N_B} |V_j| \left(G_{ij}\cos(\theta_{ij}) + B_{ij}\sin(\theta_{ij})\right) = 0 && \forall i \in N \\ &Q_{Gi} + Q_{Ci} - Q_{Di} - |V_i| \sum_{j=1}^{N_B} |V_j| \left(G_{ij}\sin(\theta_{ij}) + B_{ij}\cos(\theta_{ij})\right) = 0 && \forall i \in N \end{aligned} \tag{4}$$

where N_B denotes the number of buses. P_G, P_D are the active power output of generator and load demand, resepectively. Q_G, Q_C, and Q_D are the reactive power output of generator, shunt VAR compensator, and load demand, respectively. G_{ij} and B_{ij} are the conductance and susceptance between bus i and bus j, respectively. θ_{ij} is the voltage angle difference between bus i and bus j.

The inequality constraints represent the operation limit of the equipment (generators, transformers, shunt compensators, and security). It can be presented as:

- Generator constraints:

$$P_{Gi}{}^{min} \le P_{Gi} \le P_{Gi}{}^{max} \qquad i = 1, 2, \ldots, N_G \tag{5}$$

$$Q_{Gi}{}^{min} \le Q_{Gi} \le Q_{Gi}{}^{max} \qquad i = 1, 2, \ldots, N_G \tag{6}$$

$$V_{Gi}{}^{min} \le V_{Gi} \le V_{Gi}{}^{max} \qquad i = 1, 2, \ldots, N_G \tag{7}$$

where P_G^{max}, Q_G^{max}, and V_G^{max} denote the maximum limit of active power, reactive power, and voltage magnitude of generators, respectively. P_G^{min}, Q_G^{min}, and V_G^{min} are the minimum limit of active power, reactive power, and voltage magnitude of generators, respectively.

- Transformer constraints:

$$T_j{}^{min} \le T_j \le T_j{}^{max} \qquad j = 1, 2, \ldots, N_T \tag{8}$$

where T^{max} and T^{min} represent the maximum and minimum limit of tap regulating at transformers, respectively. N_T is the number of tap changers.

- Shunt compensator constraints:

$$Q_{C_k}{}^{min} \le Q_{C_k} \le Q_{C_k}{}^{max} \qquad k = 1, 2, \ldots, N_C \tag{9}$$

where Q^{max} and Q^{min} denote the maximum and minimum limit of the shunt compensator. N_C is the number of shunt capacitor sources.

- Security constraints:

$$V_{Li}{}^{min} \le V_{Li} \le V_{Li}{}^{max} \qquad i = 1, 2, \ldots, N_L \tag{10}$$

$$S_{L_m} \le S_{L_m}{}^{max} \qquad m = 1, 2, \ldots, N_{nl} \tag{11}$$

where S_L^{max} is the maximum limit of MVA in the transmission line. N_{nl} is the number of transmission lines.

2.3. Objective Functions

In this paper, the five most common objective functions were optimized to solve OPF problems, which are fuel cost, losses, emission, voltage deviation, and the voltage stability index.

- Total Fuel Cost [$/h]

The mathematical formulation for the total fuel cost in the power system can be expressed as follows [19]:

$$F_C = \sum_{i=1}^{N_G} f_i(P_{G_i}) = \sum_{i=1}^{N_G} \left(a_i P_{G_i}^2 + b_i P_{G_i} + c_i \right) \quad [\$/h] \tag{12}$$

a_i, b_i, and c_i denote fuel cost coefficients for generators.

- Active power losses [MW]

The second objective function in this study is active power losses in transmission lines. It can be expressed as [19]:

$$F_{loss} = \sum_{k=1}^{N_{nl}} G_i \left(V_i^2 + V_j^2 - 2 V_i V_j \cos \delta_{i,j} \right) \quad [\text{MW}] \tag{13}$$

where F_{loss} is the total real losses in transmission lines. G_i is the transfer conductance.

- Total emission [ton/h]

This objective function aims to minimize the emission level in the atmosphere by reducing pollution gases, such as NO_x and SO_2. The mathematical description of this objective function can be expressed as [7]:

$$F_{em} = \sum_{i=1}^{N_G} 10^{-2}\left(\alpha_i + \beta_i P_{G_i} + \gamma_i P_{G_i}^2\right) + \zeta_i \exp\left(\lambda_i P_{G_i}\right) \quad [\text{ton/h}] \tag{14}$$

α_i, β_i, γ_i, ζ_i, and λ_i denote fuel emission coefficients in generators.

- Voltage deviation [p.u.]

The goal of this case is to optimize the voltage quality in the system by minimizing the voltage deviations at the PQ bus from 1.0 [p.u.] The mathematical expression of this objective is expressed as [20]:

$$F_{VD} = \sum_{i=1}^{N_{PQ}} |V_i - 1.0| \quad [\text{p.u.}] \tag{15}$$

- Voltage stability index

The last objective function is to enhance the voltage stability index in the whole system by minimizing the maximum value of the voltage stability indicator (L-index). The mathematical formulation of the L-index is defined as [20]:

$$L_j = \left|1 - \sum_{i=1}^{N_G}\left(F_{ji} \times \frac{V_i}{V_j}\right)\right| \qquad j = 1, 2, \ldots, Nl \tag{16}$$

$$F_{ji} = -[Y_1]^{-1} \times [Y_2] \tag{17}$$

where Y_1 and Y_2 denote the sub-matrices of the admittance matrix (Y_{bus}). It can describe this objective function as:

$$F_{VSI} = Max(L_j) \qquad j = 1, 2, \ldots, Nl \tag{18}$$

The above objective functions are related as a single objective function, and they can be obtained by the proposed HGS approach. In addition to the single objective function, the multi-objective function was proposed to solve the multi-objective optimal power flow (MOOPF). In this article, many objective functions were optimized (they may be conflicting) simultaneously while satisfying equality and inequality constraints. Generally, a multi-objective function can be expressed by the following equation:

$$f_m(x,u) = \sum_{m=1}^{N} \omega_m f_m(x,u) = \omega_1 f_1 + \omega_2 f_2 + \ldots + \omega_m f_m \quad m = 1, 2, \ldots, N \tag{19}$$

where f denotes the MOF with No. of functions, f_m is individual OF, and ω is the weight coefficient at the ranges [0,1], N denotes the No. of OF. The sum of weight coefficients is equal to 1. In this article, the weight coefficient of each OF is inverse the number of OF. If number of OF equal 2 (Bi objective function), the weight coefficient equal to 0.5, and so on. In other words, there is no preference for any OF over the others. Therefore, we do not have any prime significance for any OF.

3. Single- and Multi-Objective OPF Frameworks

3.1. Conventional Hunger Games Search

Hunger games search (HGS) is a new optimization technique inspired by the behavior of social animal cooperatives, which is proportional to their level of hunger. The processes that characterized this algorithm into two stages can be summarized as follows:

1. Approach food

The mathematical model of this process is described as follows:

$$Y(t+1) = \begin{cases} Y(t) \cdot (1 + rand(1)), r_1 < l \\ V_1 \cdot Y_b + S \cdot V_2 \cdot |Y_b - Y(t)|, r_1 > l, r_2 > e \\ V_1 \cdot Y_b - S \cdot V_2 \cdot |Y_b - Y(t)|, r_1 > l, r_2 < e \end{cases} \tag{20}$$

where $Y(t+1)$ is the position of an individual in the next iteration; $Y(t)$ is the position of an individual in the current iteration; Y_b denotes the position of the individual chosen randomly in optimal individuals; *rand* (1), r_1, and r_2 are the random numbers within $[0, 1]$; V_1 and V_2 represent the hunger weights; S is the number within $[-a,\ a]$; l is the parameter setting experiment value; The formula of e is:

$$e = Sech(|f(i) - bf|) \tag{21}$$

where $f(i)$ denotes the fitness value; and bf is the best fitness. *Sech* is a hyperbolic function and can be described as:

$$\left(Sech(x) = \frac{2}{e^x + e^{-x}} \right) \tag{22}$$

S can be formulated as:

$$\begin{array}{l} S = 2 \times A \times r - A \\ A = 2 \times \left(1 - \frac{t}{Max_iter}\right) \end{array} \tag{23}$$

where r is a random number within $[0, 1]$; and Max_iter is the maximum iteration.

2. Hunger role

The characteristics of starvation can be expressed as a mathematical formulation as follows:

$$V_1(l) = \begin{cases} hun(i) \cdot \frac{N}{SHun} \times r_4 & r_3 < l \\ 1 & r_3 > l \end{cases} \tag{24}$$

$$V_2(l) = (1 - \exp(-|hun(i) - SHun|)) \times r_5 \times 2 \tag{25}$$

where N is the number of populations, and $SHun$ is the sum of populations that feel hunger. r_3, r_4, and r_5 are random numbers within [0, 1]. hun denotes the population's hunger and can be formulated as:

$$hun = \begin{cases} 0 & Allfitness(i) == bf \\ hun(i) + h & Allfitness(i)! = bf \end{cases}$$

$$h = \begin{cases} Lh \times (1 + r), & Th < Lh \\ Th & Th \geq Lh \end{cases} \tag{26}$$

$$Th = \frac{f(i) - bf}{wf - bf} \times r_6 \times 2 \times (ub - lb)$$

where $AllFitness(i)$ and $f(i)$ are the fitness of each population; h denotes the hunger sensation; r_6 is a random number within [0, 1]; bf and wf are the best and the worst fitness; ub and lb refer to the upper and lower bounds; and Lh is the lower bound.

To describe the process of the proposed approach, HGS, to solve optimal power flow (OPF), a pseudo-code and flowchart are presented in Algorithm 1 and Figure 1.

Algorithm 1: Pseudo-code of HGS.

Input all parameters $N,\ Max_iter, l, D, SHun$
Determine the location of population $X_i\ (i\ = 1,\ 2, \cdots,\ N)$
While $(T\ \leq\ Max_iter)$
    Calculate $f(i)$
    Update $bf,\ wf,\ Y_b,\ bl$
    Calculate the population's hunger hun by Equation (26)
    Calculate the hunger weight (1) V_1 by Equation (24)
    Calculate the hunger weight (2) V_2 by Equation (25)
    For each population
        Calculate e by Equation (21)
        Update S by Equation (22)
        Update location by Equation (20)
    End (For)
    $T = T + 1$
End (While)
Return $bf,\ Y_b$

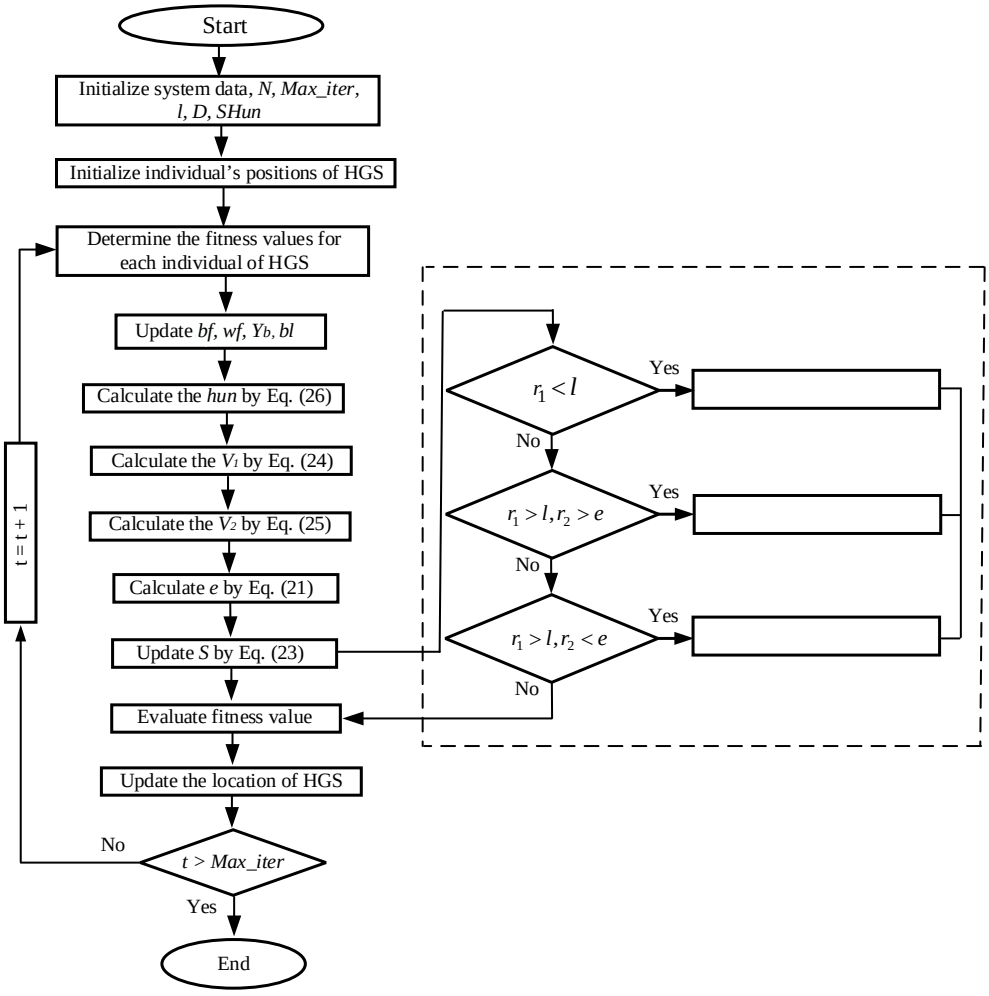

Figure 1. Flowchart of the HGS.

3.2. Multi-Objective Hunger Games Search (MOHGS)

A new approach was proposed to solve MOOPF problems (two or more objective functions) and optimize simultaneously, namely, the multi-objective hunger games search (MOHGS). Based on the number of objective functions, the Pareto concept (PC) is the proposed approach to find out the dominant and non-dominated solutions. The decision

maker is responsible to determine the best compromise solution (BCS) from non-dominated solutions (NDS). Many approaches were suggested to determine the BCS, such as the fuzzy set theory, entropy criterions, and centroid concept [21]. The most popular approach used to find out the BCS is the fuzzy decision maker [21–24]. In this study, the fuzzy membership function (FMF) is the equation used to extract the BCS from NDS. Finally, the specific strategy that is employed to reduce and arrange the NDPF is the crowding distance (CD).

1. Pareto concept (PC)

The Pareto concept (PC) is the method used to find the NDS. In general, a solution x_1 dominates solution x_2 when:

$$\begin{array}{l} \forall i \in \{1, 2, \ldots, n\} : f_i(x_1) \leq f_i(x_2) \\ \forall j \in \{1, 2, \ldots, n\} : f_j(x_1) < f_j(x_2) \end{array} \quad (27)$$

2. The best compromise solution (BCS)

The equation below is used to determine the BCS based on fuzzy membership function (FMF) (Figure 2).

$$u_i^k = \begin{cases} 1 & F_i \leq F_i^{min} \\ \frac{F_i^{max} - F_i}{F_i^{max} - F_i^{min}} & F_i^{min} < F_i < F_i^{max} \\ 0 & F_i \geq F_i^{max} \end{cases} \quad (28)$$

$$u^k = \frac{\sum_{i=1}^{N_{obj}} u_i^k}{\sum_{k=1}^{M} \sum_{i=1}^{N_{obj}} u_i^k} \quad (29)$$

where F_i^{min} and F_i^{max} represent the minimum and maximum values of NDS. u_i^k denotes the normalized membership function of each NDS. u^k is the BCS when having the maximum value [25].

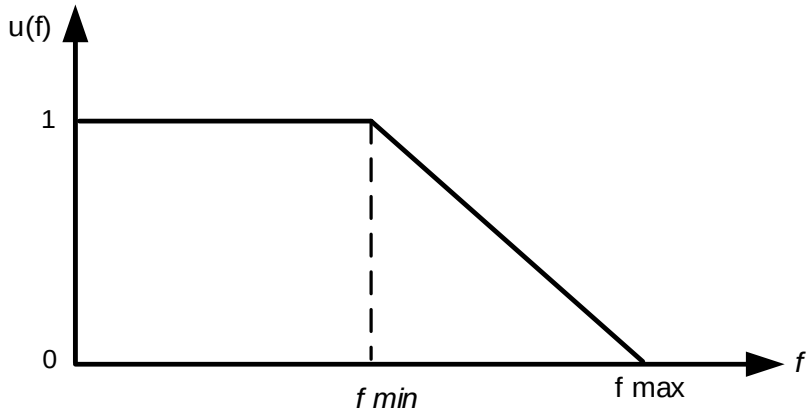

Figure 2. The membership functions.

3. Crowding distance strategy

This strategy is employed to rank and reduce NDS in NDPF. The average of two neighboring NDS represents the value of crowding distance (CD). First, the fitness of for each population should be sorted in a descending order. Thereafter, the boundary solutions are determined as an infinite value for each objective function. For the remainder solutions, the corresponding diagonal length of the intermediate solutions is assigned. Figure 3

represents the CD of an individual solution as the diagonal length of the cuboid. It is expressed as follows:

$$cd_i = \prod_{n=1}^{m} \frac{|f_n(x_i + 1) - f_n(x_i - 1)|}{f_{n,min}}, \qquad i = 1, 2, \cdots, n_b \tag{30}$$

where cd_i represents the crowding distance; $F_{n,\,min}$ denotes the minimum value of the nth objective function; N_b is the No. of candidate solutions.

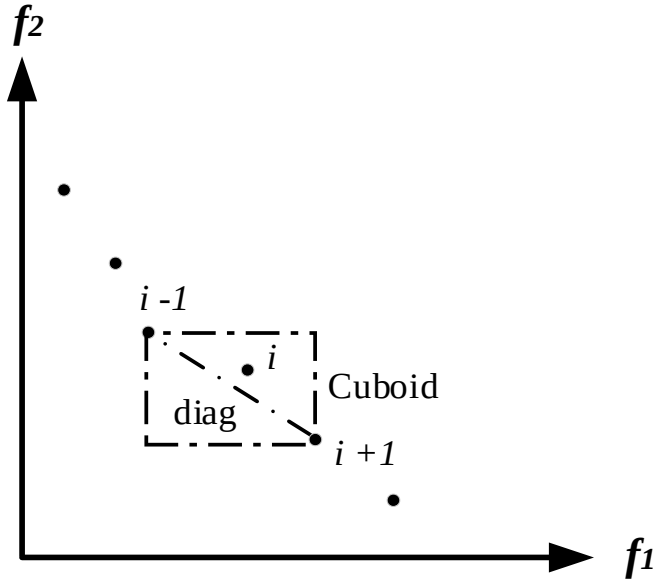

Figure 3. The crowding distance estimation.

4. Stages of multi-objective HGS

The phases of MOHGS can be summarized as follows:

Step 1: Initialize system data such as max iteration, No. of population, the sum of populations that feel hunger, No. of NDS, No. of control variables, the parameter setting experiment, etc.

Step 2: Initialize individual's positions in the HGS.

Step 3: Calculate fitness values for each individual in the HGS.

Step 4: Sort NDS according to the fitness value and store it in the initial repository.

Step 5: Calculate the best and the worst fitness, the upper and lower bounds, and the position individual is chosen randomly.

Step 6: Calculate the *hun* by (25).

Step 7: Calculate e, S, and the hunger weights (V_1 *and* V_2) by (20), (22), (23), and (24).

Step 8: Update the position of the individual in the next iteration (Y(t+1)), based on (19).

Step 9: Calculate the fitness value of each HGS.

Step 10: Update the position of HGS.

Step 11: Sort the NDS of HGS and store it in the HGS repository.

Step 12: Combine the NDS in the initial and HGS repository with the NDS of the HGS, updated to find new NDS.

Step 13: The stopping criteria, if the number of non-dominated solutions is equal to 500, end. Otherwise, store the non-dominated solutions in the initial repository, return to step 3.

The processes used to solve MOOPF problems with the developed approach MOHGS can be expressed in Figure 4.

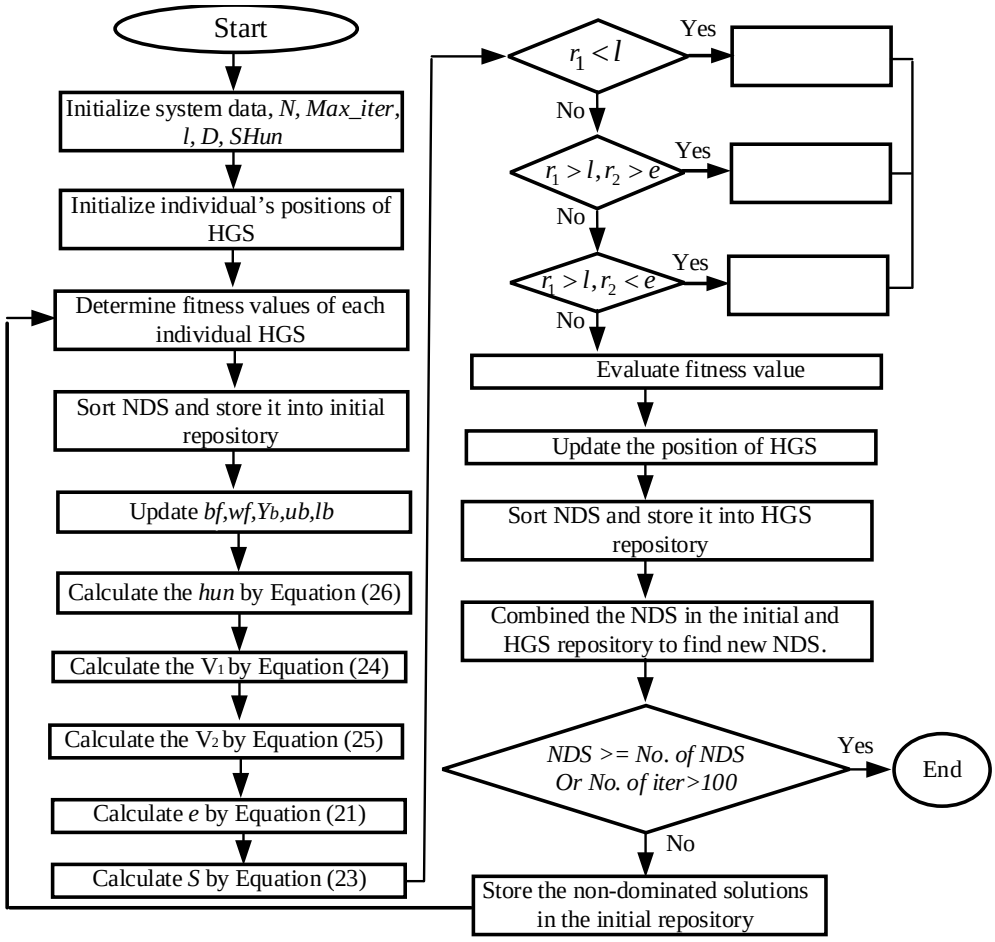

Figure 4. Flowchart of MOHGS.

4. Simulation Results and Discussion

In this study, two bus power systems were tested, IEEE 30 and IEEE 57 bus, and twenty-five case studies were investigated to prove the viability and efficiency of the proposed approaches (HGS and MOHGS). Table 1 presents the characteristics of these systems. The cases studied are summarized in Table 2. The simulation results were carried out on Intel Core (TM) i5-10500H 2.5GHz (12 CPUs) and 16384 (64 bit) MB RAM. The active power output of the generator without the slack bus, the voltage of the generator bus, tap setting regulating of transformers, and shunt capacitors VAR, which are connected on transmission lines, are the control variables that were set to obtain the optimal objective function.

4.1. IEEE 30-Bus Power System

In this article, the IEEE 30-bus system represents the first test system that was applied to validate the effectiveness and superiority of the proposed approaches (HGS and MOHGS), as shown in Figure 5. The control variable for the OPF problem for the IEEE 30-bus system is 24. The cost and emission coefficients of this system are illustrated in Table 3. The maximum and minimum limits of voltage magnitude for generators and load bus are in the range [0.9–1.1] and [0.95–1.05], respectively.

4.1.1. Single-Objective OPF

Five objective functions were applied to demonstrate the efficiency and superiority of the proposed algorithm HGS. In a single OF, the objective functions that are optimized are total fuel cost [$/h], total emission [ton/h], active power losses [MW], voltage deviation [p.u.], and voltage stability index. The parameters chosen to solve a single OF are 1000 iterations and 250 population size.

Table 1. The main characteristics of the systems.

System Characteristics	IEEE 30-Bus	IEEE 57-Bus
Buses	30	57
Branches	41	80
Generators	9 (Buses:1, 2, 5, 8, 11, and 13)	7 (Buses: 1, 2, 3, 6, 8, 9, 12)
Generator voltage limits	0.90–1.1 [p.u.]	0.90–1.1 [p.u.]
Load voltage limits	0.95–1.05 [p.u.]	0.94–1.06 [p.u.]
Limit of tap changer setting	0.90–1.1 [p.u.]	0.90–1.1 [p.u.]
Limit of VAR	0–5 [p.u.]	0–20 [p.u.]
Shunts	9 (Buses: 10, 12, 15, 17, 20, 21, 23, 24, and 29)	3 (Buses: 18, 25, 53)
Transformers	4 (Buses: 11, 12, 15, and 36)	17 (Buses: 19, 20, 31, 35, 36, 37, 41, 46, 54, 58, 59, 65, 66, 71, 73, 76, 80)
MW demand	283.4 [MW]	1250.8 [MW]
Control variables	24	33

Table 2. The studied cases with different types.

System	Type of OF(s)	Case #	FC	Em	APL	VD	VSI
IEEE 30-bus	Single OF (s)	#1	√				
		#2			√		
		#3		√			
		#4				√	
		#5					√
	Bi-OF(s)	#6	√	√			
		#7	√		√		
		#8	√			√	
		#9	√				√
		#10		√		√	
		#11			√	√	
		#12				√	√
	Triple-OF(s)	#13	√	√	√		
		#14	√	√		√	
		#15	√		√	√	
		#16	√	√		√	
		#17	√		√		√
		#18	√	√			√
		#19	√			√	√
	Quad-OF(s)	#20	√	√	√	√	
		#21	√	√	√		√
	Quinta-OF(s)	#22	√	√	√	√	√
IEEE 57-bus	Single OF (s)	#23	√				
		#24		√			
		#25			√		

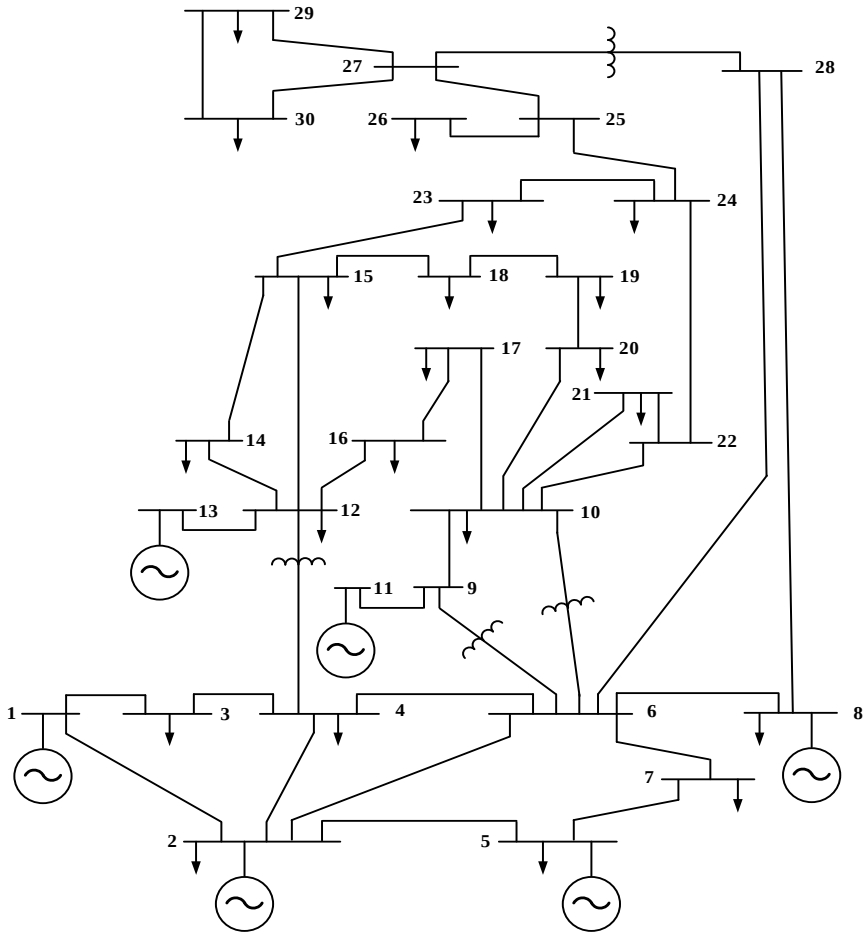

Figure 5. Single-line diagram of the IEEE 30 bus system.

Table 3. The cost and emission coefficients of generators for the IEEE 30 bus system.

	Coefficient Generating Unit					
	G1	G2	G5	G8	G11	G13
	Fuel cost coefficient					
a	0	0	00	0	0	0
b	2	1.75	1	3.25	3	3
c	0.00375	0.0175	0.0625	0.00834	0.025	0.025
	Emission coefficient					
α	4.091	2.543	4.258	5.326	4.258	6.131
β	−5.554	−6.047	−5.094	−3.55	−5.094	−5.555
γ	6.49	5.638	4.586	3.38	4.586	5.151
ζ	2.00×10^{-4}	5.00×10^{-4}	1.00×10^{-6}	2.00×10^{-3}	1.00×10^{-6}	1.00×10^{-5}
λ	2.857	3.33	8	2	8	6.67

Case #1: In this case, the rate of fuel cost minimization [$/h] is the objective function that was optimized by the HGS algorithm. The convergence plot of fuel cost [$/h] for the IEEE 30 bus system is depicted in Figure 6a. The total fuel costs are reduced from 901.6391 [$/h] (initial case) to 799.2202 [$/h] (best case) with a reduction loss of 11.36%, as listed in Table 4.

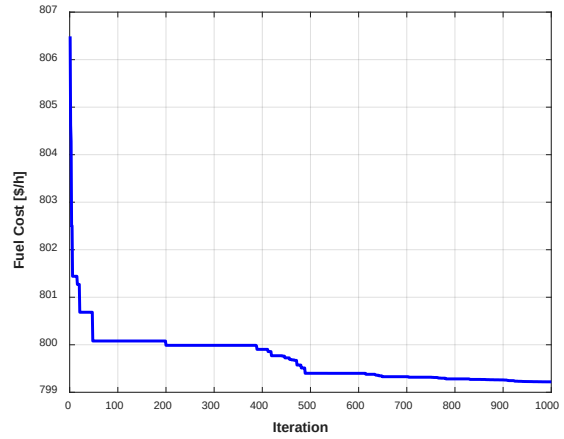

(**a**) Case #1

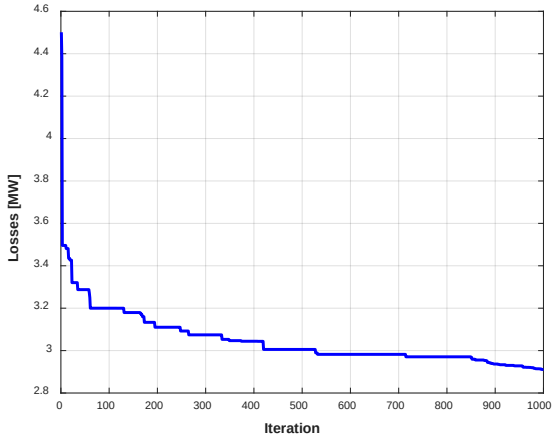

(**b**) Case #2

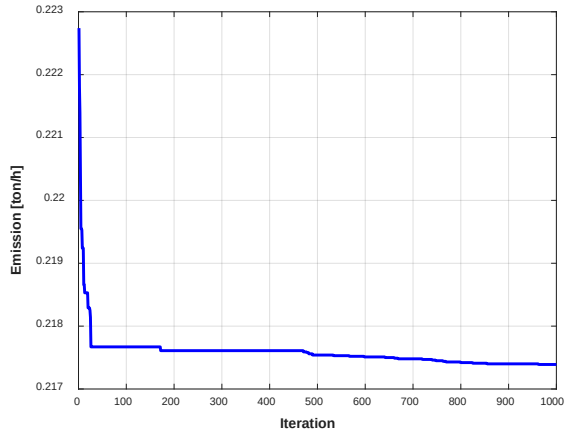

(**c**) Case #3

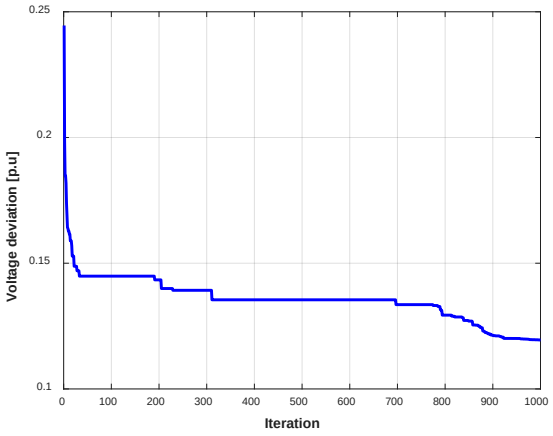

(**d**) Case #4

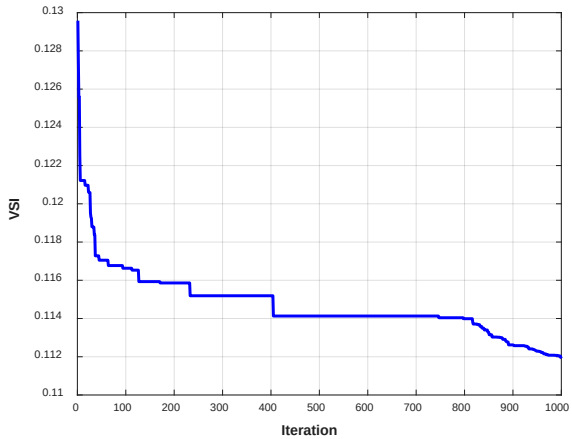

(**e**) Case #5

Figure 6. Convergence plots obtained by HGS for cases #(1–5).

Table 4. The best control variables obtained by HGS for cases #(1–5).

Item		Limit		Initial [26]	Case				
		Max	Min		#1	#2	#3	#4	#5
[MW]	P_1	50	200	99.223	176.73	51.518	67.9326	99.3206	75.4018
	P_2	20	80	80	48.6285	79.9472	71.0846	56.2324	72.3195
	P_5	15	50	50	21.3556	49.9963	49.999	48.5423	49.6165
	P_8	10	35	20	20.9611	34.8738	34.999	34.7508	32.8099
	P_{11}	10	30	20	12.3146	29.9886	29.9995	19.9674	28.8962
	P_{13}	12	40	20	12.047	39.9871	32.7369	29.7117	27.9364
[p.u.]	V_1	0.95	1.1	1.05	1.10	1.09957	1.07979	1.00733	1.09893
	V_2	0.95	1.1	1.04	1.0879	1.09575	1.02963	0.99464	1.09953
	V_5	0.95	1.1	1.01	1.08115	1.07676	1.06095	1.06787	1.09397
	V_8	0.95	1.1	1.01	1.08895	1.09501	1.09796	1.05785	1.09956
	V_{11}	0.95	1.1	1.05	1.09935	1.09985	1.09540	1.05771	1.09950
	V_{13}	0.95	1.1	1.05	1.09998	1.09975	1.06955	0.99197	1.09772
[MVAr]	Q_{c10}	0	5	0	4.40056	4.21049	4.05070	3.89253	4.96503
	Q_{C12}	0	5	0	4.24071	4.19982	3.13443	1.68208	2.09009
	Q_{c15}	0	5	0	4.47918	4.26252	3.70849	2.33112	4.61987
	Q_{17}	0	5	0	4.98546	4.31378	3.62262	3.14785	3.53632
	Q_{c20}	0	5	0	4.62076	4.26326	4.13636	4.99605	4.95659
	Q_{21}	0	5	0	4.97743	4.27526	1.42028	4.06093	4.94313
	Q_{c23}	0	5	0	4.41930	4.16337	2.22773	4.97509	4.66820
	Q_{24}	0	5	0	4.98744	4.23189	4.69879	4.99004	4.99429
	Q_{29}	0	5	0	3.78063	4.03580	3.42316	2.55515	4.99515
Tap Position	T_{11}	0.9	1.1	1.078	1.02609	1.01962	1.03789	0.97665	1.04588
	T_{12}	0.9	1.1	1.069	0.99766	1.04051	1.02467	0.98726	1.03403
	T_{15}	0.9	1.1	1.032	0.99149	0.95436	1.02072	0.99930	0.95605
	T_{36}	0.9	1.1	1.068	0.98371	0.99075	1.01205	0.96666	0.95025
Fuel cost [$/h]				901.639	**799.220**	966.837	933.703	889.278	920.183
Active power loss [MW]				5.6891	8.6424	**2.9109**	3.3515	5.1253	3.5803
Emission [ton/h]				0.2253	0.3673	0.2216	**0.2174**	0.2343	0.2204
Voltage deviation [p.u.]				1.1747	1.5671	1.7078	0.7971	**0.1195**	1.9699
Voltage stability index				0.1727	0.1199	0.1191	0.1314	0.1375	**0.1119**
Reduction rate				-	11.36%	48.83%	3.51%	89.83%	35.20%
Average resolution time [s/iter]				-	1.4834	1.631	1.613	1.575	1.609

The bold represents the best values of OF.

Case #2: The main aim of this case was to reduce the active power loss [MW] in the transmission lines using the HGS algorithm. The reduction rate in losses is 48.83% (reducing from 5.6891 [MW] to 2.9109 [MW]). The convergence speed of this case is illustrated in Figure 6b.

Case #3: Due to increasing environmental pollution, the new studies drew growing attention in emission. In this paper, this objective function deals with emission minimization. The variations of emission over iteration are described in Figure 6c. The best value of emission that can be achieved by the HGS algorithm is 0.2174 [ton/h]. The total emissions are reduced from 0.2253 [ton/h] to 0.2174 [ton/h] with a reduction rate equal to 3.51%, as illustrated in Table 4.

Case #4: To improve the voltage at PQ bus, the voltage deviation is the objective function that is considered. The sum voltage deviation reduced from 1.1747 to 0.1195 (reduction rate is 89.83%), as seen in Table 4. The convergence speed for this case is shown in Figure 6d.

Case #5: The fifth objective function is to enhance voltage stability of the whole system by minimizing the maximum value of the voltage stability indicator (L-max) using the HGS algorithm. The convergence characteristics of VSI using the proposed approach of HGS is depicted in Figure 6e. The reduction rate of this case is equal to 35.20% (compared between

the initial case, which is 0.1727, and the optimal case using HGS, which is 0.1119) as given in Table 4.

The best control variables for cases (1–5) using the proposed algorithm HGS on the IEEE 30 bus system are depicted in Table 4. To prove the superiority and effectiveness of the performance of the HGS algorithm, the best results obtained by the HGS algorithm for fuel cost [$/h], active power losses [MW], emission [ton/h], voltage deviation [p.u.], and voltage stability index are compared with other recent optimization methods results reported in the literature, as seen in Tables 5 and 6. The bold line represents the best values of OF obtained by HGS.

Table 5. Comparison of the best results obtained by HGS with other algorithms for cases (1,2).

Case #1		**Case #2**	
Method	**FC [$/h]**	**Method**	**APL [MW]**
Initial	901.6391	Initial	5.830
SCA [27]	800.1018	SSO [28]	3.8239
DSA [29]	800.3887	EM [30]	3.1775
JAYA [31]	800.479	GPU-PSO [32]	3.2601
MSA [33]	800.5099	EGA-DQLF [34]	3.2008
SP-DE [35]	800.4131	ASO [36]	3.1600
MGOA [37]	800.4744	EGA-EA [38]	3.2601
AMTPG-Jaya [39]	800.1946	GWO [10]	4.2905
TLBO [39]	800.4604	PSO [40]	5.1957
ABC [41]	800.6850	HPSO-DE [40]	5.1476
IABC [41]	800.4215	FAHSPSO-DE [40]	4.9989
SSO [28]	802.2580	IPSO [42]	5.0732
GPU-PSO [32]	800.53	HHO [43]	3.49
EGA [44]	802.06	SSA [43]	3.50
IGA [45]	800.805	WOA [43]	3.50
AGAPOP [46]	799.8441	MF [43]	3.50
ABC [47]	800.66	GWO [43]	3.51
PSOGSA [48]	800.49859	SMA [14]	2.9934
GWO [10]	802.7924	HGS	**2.9109**
ISSA [49]	800.4752		
MFO [49]	800.7134		
IHS [49]	800.5202		
GA [49]	800.5272		
SOS [50]	801.5733		
SMA [14].	799.2557		
HGS	**799.2202**		

The bold line represents the best values of OF obtained by HGS.

Table 6. Comparison of the best results obtained by HGS with other algorithms for cases (3–5).

Case #3		**Case #4**		**Case #5**	
Method	**Em [ton/h]**	**Method**	**VD [p.u]**	**Method**	**VSI**
Initial	0.3661	Initial	1.1747	Initial	0.1727
BSA [51]	0.2425	HFPSO [52]	0.1467	Jaya [31]	0.1243
SSO [28]	0.2315	EJADE-SP [9]	0.3752	AMTPG-Jaya [39]	0.1240
HHO [43]	0.2850	MABC [53]	0.1292	SSO [28]	0.1267
SSA [43]	0.2950	HGS	**0.1195**	NISSO [28]	0.12547
WOA [43]	0.2950			TLBO [39]	0.12444
MF [43]	0.2950			ARCBBO [54]	0.1369
GWO [43]	0.2960			ECHT-DE [55]	0.13632
SMA [14]	0.2175			SPEA [56]	0.1247
HGS	**0.2174**			DE [57]	0.1246
				SMA [14]	0.1136
				HGS	**0.1119**

The bold represents the best values of objective OF obtained by the HGS.

4.1.2. Bi-Objective OPF

In this subsection, two objective functions were optimized simultaneously to achieve the best compromise solution (BCS) of non-dominated solutions (NDS). The function used to find the BCS was the fuzzy membership function (FMF). The crowding distance (CD) was the method employed to rank and reduce NDS of the NDPF. The developed approach MOHGS was applied in power systems to demonstrate its performance to solve MOOPF problems. In this subsection, seven case studies were suggested to prove the efficiency and superiority of the MOHGS. The population size was 500 pollinators; the program was stopped when the number of NDS was equal to the number of NDS suggested, which was 500, or a number of iterations equal to 100 iterations. These cases can be summarized as follows:

Case #6: In the first case of Bi-OF, the total fuel cost and total emission were optimized simultaneously by using the proposed approach MOHGS. The BCS of fuel cost and emission were 827.735 [$/h] and 0.2587 [ton/h], respectively.

Case #7: The second case of this type, the total fuel cost and active power losses were considered as objective functions and optimized simultaneously. The BCS of fuel cost and losses were 826.842 [$/h] and 5.5946 [MW].

Case #8: The third case of bi-objectives functions that were optimized in this work were fuel cost and voltage deviation. The BCS of fuel cost and voltage deviation are 803.094 [$/h] and 0.1813 [p.u.]

Case #9: The fuel cost and voltage stability index are the objective functions that were minimized simultaneously in this case. The BCS was 801.491 [$/h] and 0.1213 of fuel cost and voltage stability index, respectively.

Case #10: The fifth case of Bi-OF was minimizing the total emission and voltage deviation simultaneously. The BCS of emission and voltage deviation were 0.2245 [ton/h] and 0.1508 [p.u.].

Case #11: The active power losses and voltage deviation represented the objective functions that were optimized simultaneously in this case. The BCS of losses and voltage deviation were 3.8636 [MW] and 0.2048 [p.u.].

Case #12: The voltage deviation and voltage stability index represented the last case of Bi objective OPF. The BCS of voltage deviation and voltage stability index were 0.3690 [p.u.] and 0.1280.

Figure 7a–g shows Pareto front solutions of the bi-objective functions obtained by the MOHGS on the IEEE 30-bus system. The best compromise solution of Bi OF for cases 6–12 is indicated by red diamonds, as shown in Figure 7.

4.1.3. Triple Objective OPF

In this type, three objective functions were considered simultaneously to obtain the BCS from NDS in the NDPF. Seven case studies are proposed; the population size is 500 pollinators. The stopping criteria of simulation running when the number of iterations equal to 100 iterations, or the number of non-dominated solutions equal to 500 pollinators. These cases can be summarized as follows:

Case #13: In the first case in this type, the fuel cost, emission, and losses combined were optimized simultaneously by using the proposed approach MOHGS to achieve the Pareto set solutions. The BCS of fuel cost, emission, and losses were 845.2988 [$/h], 0.2416 [ton/h], and 5.0562 [MW], respectively.

Case #14: In this case, the fuel cost, emission, and voltage deviation were considered objective functions and optimized simultaneously. The BCS of fuel cost, emission, and voltage deviation were 825.1766 [$/h], 0.2667 [ton/h], and 0.1953 [p.u.], respectively.

Case #15: The third case of triple-objective functions were minimization of fuel cost, losses, and voltage deviation. The BCS of fuel cost, losses, and voltage deviation were 817.1199 [$/h], 7.3484 [MW], and 0.1767 [p.u.], respectively.

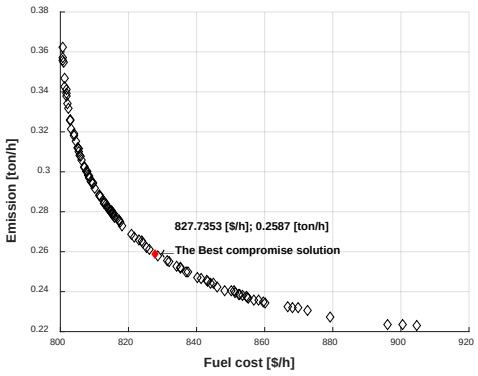

(**a**) Case #6

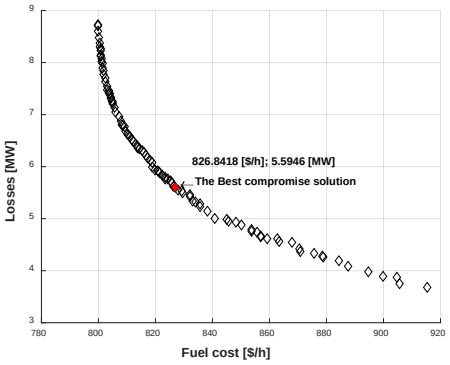

(**b**) Case #7

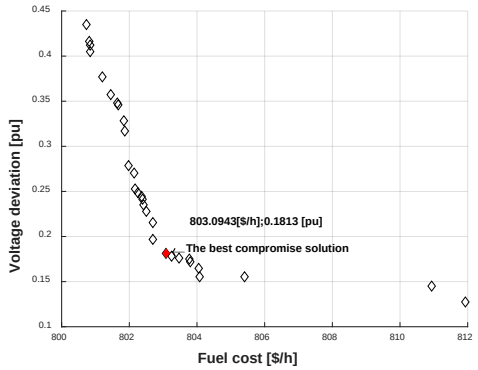

(**c**) Case #8

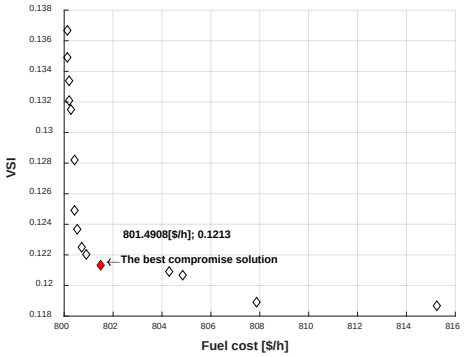

(**d**) Case #9

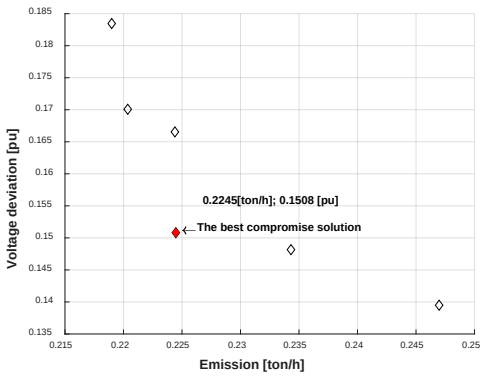

(**e**) Case #10

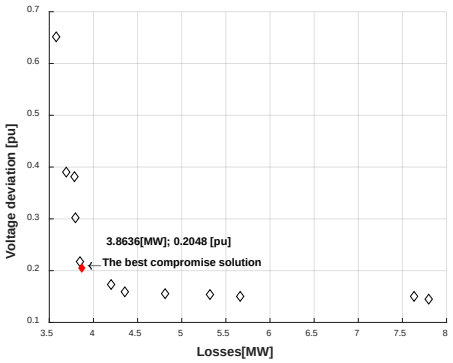

(**f**) Case #11

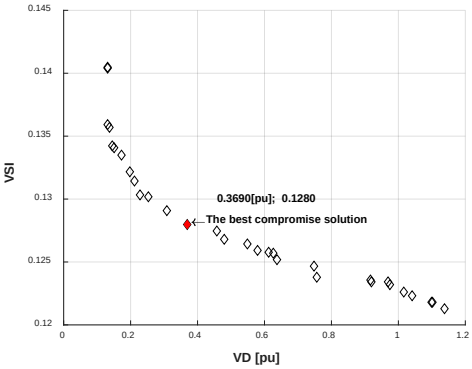

(**g**) Case #12

Figure 7. The Pareto fronts obtained by MOSMA for cases #(6–12).

Case #16: The active power losses, emission, and voltage deviation were the objective functions that were optimized simultaneously. The BCS was 3.8246 [MW], 0.2196 [ton/h], 0.2122 [p.u.] for losses, emission, and voltage deviation, respectively.

Case #17: The seventeenth case in this paper was minimization in fuel cost, losses, and voltage stability index, simultaneously. The BCS of fuel cost, losses, and voltage stability index were 834.4639 [$/h], 5.4740 [MW], 0.1198, respectively.

Case #18: In this case, the objective functions that were optimized included the fuel cost, emission, and voltage stability index. The BCS of fuel cost, losses, and voltage stability index were 835.0571 [$/h], 0.2504 [ton/h], 0.1192, respectively.

Case #19: Fuel cost, voltage deviation, and voltage stability index were the objective functions that were minimized simultaneously. The BCS of fuel cost, voltage deviation, and voltage stability index were 802.5842 [$/h], 0.4813 [p.u.], 0.1279, respectively.

The three-dimensional Pareto fronts set that were obtained by the developed approach MOHGS are illustrated in Figure 8a–g. The best compromise solutions of Tri OF for cases 13–19 are indicated by red diamonds, as shown in Figure 8.

4.1.4. Quad and Quinta Objective OPF

The last type of objective functions applied on the IEEE 30-bus system represents the Quad and Quinta objective functions. Two case studies on Quad objective functions and one case study on Quinta objective function are the suggested cases to solve MOOPF in this type. The stopping criteria are achieved when the No. of NDS is equal to 500 pollinators, or the No. of iterations reaches 500. It can be summarized as follows:

Case #20: Total fuel cost, losses, emission, and voltage deviation are the objective functions that were optimized in this case. The BCS obtained by MOHGS were 845.4721 [$/h], 5.7458 [MW], 0.2507 [ton/h], and 0.1400 [p.u.] for fuel cost, losses, emission, and voltage deviation., respectively.

Case #21: The objective functions that were optimized simultaneously were fuel cost, losses, emission, and voltage stability index. The BCS were 819.4061 [$/h], 7.4137 [MW], 0.2898 [ton/h], and 0.1389 for fuel cost, losses, emission, and voltage stability index, respectively.

Case #22: In this case, five objective functions were optimized simultaneously, which were fuel cost, losses, emission, voltage deviation, and voltage stability index. The best results of objective functions obtained by MOHGS were 818.7575 [$/h], 7.4471 [MW], 0.2912 [ton/h], 0.3272 [p.u.], and 0.1399 for fuel cost, losses, emission, voltage deviation, and voltage stability index, respectively.

Tables 7 and 8 represent the better control variables obtained by MOHGS for Bi, Tri, Quad, and Quinta objective functions that are illustrated by cases (20–22).

The voltage profiles at each load bus are charted in Figure 9a. From Figure 9a, it can be concluded that the voltage magnitude in the load bus for cases (1, 2, 3, and 5) exceeds the maximum limit (1.05 [p.u.]) for some buses, while the voltage magnitude of PQ bus for case 4 (when the voltage deviation is considered as an objective function) have not exceeded the minimum and maximum limit (0.95–1.05) [p.u.]). In Bi objective functions, the voltage profiles of this type are illustrated in Figure 9b. The numerical results obtained by MOHGS illustrate that the voltage magnitude of PQ bus exceeds the maximum limit in cases when the voltage deviation is not considered an objective function (cases (1,2,4)). However, the voltages magnitude has not exceeded the minimum and maximum limit for the cases in which the voltage deviation is considered an objective function (cases 3,5,6,7)). Figure 9c illustrates that the voltage magnitude values of some buses in cases 8, 12, 13 (the cases where the voltage deviation is not considered an objective function) exceed the maximum [1.05 p.u.], while the voltage magnitude values in cases (9, 10, 11, 14) have not exceeded the minimum and maximum limit [0.95–1.05 p.u.]. The voltage profiles for types Quad and Quinta are illustrated in Figure 9d. Figure 9d illustrates that the voltage magnitude of the load bus for these cases has not violated the boundary limit [0.95–1.05] [p.u.].

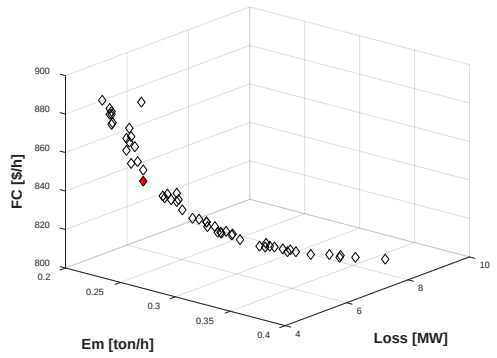

(**a**) Case #13

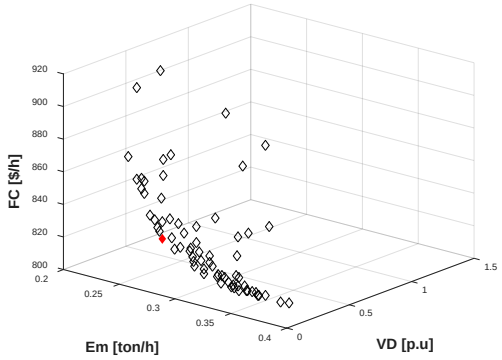

(**b**) Case #14

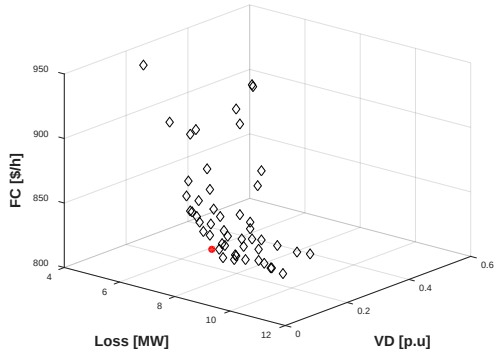

(**c**) Case #15

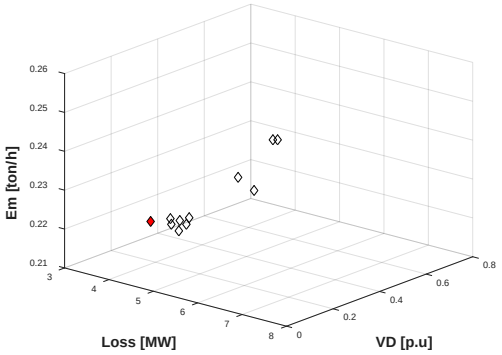

(**d**) Case #16

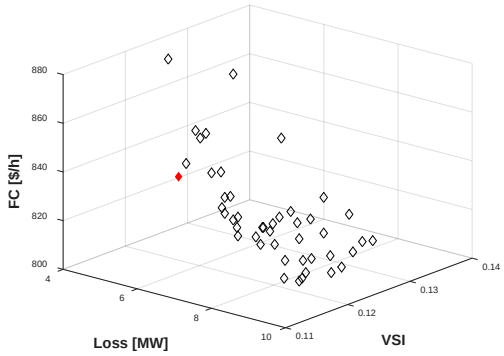

(**e**) Case #17

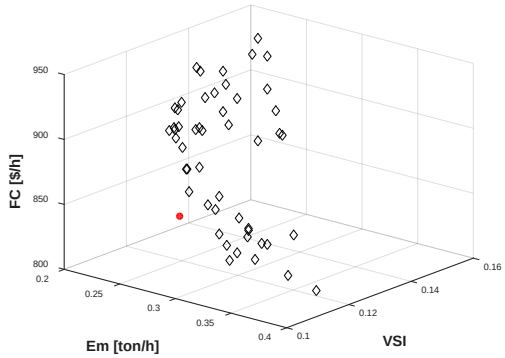

(**f**) Case #18

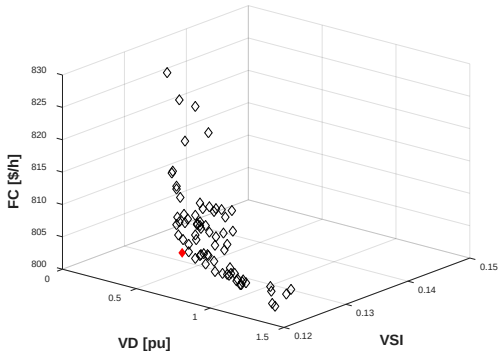

(**g**) Case #19

Figure 8. The Pareto fronts obtained by MOSMA for cases #(13–19).

Table 7. Better control variables obtained by HGS for cases (6−15).

Item		Case									
		#6	**#7**	**#8**	**#9**	**#10**	**#11**	**#12**	**#13**	**#14**	**#15**
[MW]	P_1	120.99	125.59	177.232	176.954	87.646	62.266	145.554	107.558	127.609	141.273
	P_2	60.834	48.558	46.335	44.891	64.306	75.233	78.062	61.963	59.373	52.885
	P_5	28.719	27.875	21.539	18.819	47.005	48.636	24.003	32.594	26.056	29.708
	P_8	34.476	34.619	21.650	21.417	34.672	32.980	18.529	33.168	34.366	30.809
	P_{11}	21.773	26.675	13.122	14.813	27.983	29.414	10.806	29.236	27.365	22.131
	P_{13}	22.520	25.678	13.130	15.373	26.889	38.735	15.923	23.937	15.486	13.942
[p.u.]	V_1	1.092	1.097	1.051	1.095	1.003	1.031	1.053	1.097	1.072	1.068
	V_2	1.053	1.099	1.015	1.099	1.026	1.060	1.043	1.086	1.000	1.047
	V_5	1.093	1.063	1.053	1.099	1.076	1.002	0.972	1.082	1.068	1.040
	V_8	1.055	1.077	1.061	1.084	1.063	1.054	1.097	1.068	1.037	1.004
	V_{11}	1.095	1.099	1.037	1.085	0.986	1.040	1.083	1.099	1.055	1.037
	V_{13}	1.090	1.076	1.085	1.082	1.028	1.010	1.052	1.073	1.015	0.979
[MVAr]	Q_{c10}	1.354	2.316	3.047	2.628	1.773	0.075	3.266	0.699	0.658	0.688
	Q_{C12}	0.804	2.958	0.160	2.868	1.243	0.000	0.278	3.942	0.730	4.276
	Q_{c15}	3.354	0.888	4.338	0.836	0.512	0.240	4.486	0.400	1.395	0.405
	Q_{17}	2.167	2.201	0.342	3.719	2.748	0.188	3.587	2.653	0.360	0.627
	Q_{c20}	1.133	1.648	3.588	3.687	1.528	0.782	3.673	1.737	1.704	4.744
	Q_{21}	0.261	1.228	4.004	3.411	2.983	4.688	3.797	2.421	0.715	1.176
	Q_{c23}	0.503	2.613	3.848	1.022	3.508	4.964	1.118	4.808	1.550	0.123
	Q_{24}	0.908	3.930	2.127	4.944	4.474	1.196	4.449	1.649	4.883	4.128
	Q_{29}	1.623	1.035	0.545	4.305	0.898	0.893	4.948	2.707	4.010	1.663
Tap Position	T_{11}	0.977	1.038	1.057	0.965	0.972	0.961	1.043	0.993	0.970	0.952
	T_{12}	0.962	0.983	0.971	0.974	0.950	0.963	1.098	0.972	0.978	0.971
	T_{15}	1.060	1.054	0.958	1.009	0.968	0.984	0.989	1.088	0.959	0.950
	T_{36}	1.000	0.997	0.955	0.953	0.954	0.951	0.951	0.972	0.973	0.954
GFC [$/h]		**827.74**	**826.84**	**803.094**	**801.491**	899.074	946.099	826.338	**845.299**	**825.177**	**817.12**
RPL [MW]		5.9178	**5.5946**	9.6092	8.8720	5.1007	**3.8636**	9.4757	**0.2416**	6.8612	**7.3484**
Em [ton/h]		**0.2587**	0.2619	0.3678	0.3668	**0.2245**	0.2208	0.3077	**5.0562**	**0.2667**	0.2868
VD [p.u.]		0.8944	0.9559	**0.1813**	1.3536	**0.1508**	**0.2048**	**0.3690**	1.0547	**0.1953**	**0.1767**
VSI		0.1373	0.1333	0.1410	**0.1213**	0.1413	0.1445	**0.1280**	0.1282	0.1392	0.1412
Average resolution time [s/iter]		2.723	4.7027	2.7262	2.6784	2.70	2.68	2.703	2.79	2.734	2.718

The bold represents the BCS of OF.

Table 8. The better control variables obtained by HGS for cases (16–22).

Item		Case						
		#16	**#17**	**#18**	**#19**	**#20**	**#21**	**#22**
[MW]	P_1	67.936	121.170	113.261	179.444	119.182	142.724	143.244
	P_2	68.222	55.959	65.029	45.132	48.973	52.684	57.063
	P_5	49.162	34.921	29.736	19.931	40.045	33.242	32.352
	P_8	34.370	33.035	34.654	23.632	24.910	29.195	24.328
	P_{11}	29.153	27.184	22.918	11.624	18.664	16.913	20.928
	P_{13}	38.381	16.605	23.210	13.170	39.105	16.055	12.932
[p.u.]	V_1	1.015	1.083	1.099	1.086	1.006	1.052	1.074
	V_2	0.987	1.076	1.090	1.087	1.086	0.998	1.004
	V_5	1.032	1.099	1.079	1.026	1.088	1.005	1.026
	V_8	1.048	1.087	1.093	1.099	1.097	1.093	1.076
	V_{11}	1.094	1.083	1.087	0.980	0.996	1.096	1.013
	V_{13}	1.071	1.096	1.091	0.990	1.084	1.085	0.981

Table 8. *Cont.*

Item		Case						
		#16	**#17**	**#18**	**#19**	**#20**	**#21**	**#22**
[MVAr]	Q_{c10}	2.414	3.784	4.171	3.803	0.229	2.182	0.888
	Q_{C12}	2.485	3.543	1.272	4.502	1.402	1.709	1.529
	Q_{c15}	3.754	4.974	1.142	0.108	2.792	4.237	3.093
	Q_{17}	0.880	1.844	0.188	0.204	1.085	0.831	1.063
	Q_{c20}	1.670	4.075	2.411	0.782	0.612	4.614	0.894
	Q_{21}	0.349	4.448	4.984	4.005	3.912	2.728	3.500
	Q_{c23}	1.894	2.264	4.077	2.077	4.720	3.717	2.649
	Q_{24}	4.431	3.851	3.015	4.868	3.889	0.812	2.482
	Q_{29}	0.494	3.948	4.108	4.796	2.432	3.919	3.497
Tap Position	T_{11}	1.010	0.950	0.959	0.998	1.044	1.012	0.963
	T_{12}	0.981	1.026	0.980	0.979	0.976	1.075	1.024
	T_{15}	1.001	0.962	0.974	1.003	0.984	0.957	0.993
	T_{36}	0.963	0.954	0.953	0.952	1.028	1.013	0.976
GFC [$/h]		936.4713	**834.4639**	**835.0571**	**802.5842**	**845.4721**	**819.4061**	**818.7575**
RPL [MW]		**3.8246**	**5.4740**	5.4107	9.5336	**5.7458**	**7.4137**	**7.4471**
Em [ton/h]		**0.2196**	0.2559	**0.2504**	0.3746	**0.2507**	**0.2898**	**0.2912**
VD [p.u.]		**0.2122**	1.5161	1.6370	**0.4813**	**0.1400**	0.3514	**0.3272**
VSI		0.1444	**0.1198**	**0.1192**	**0.1279**	0.1456	**0.1389**	**0.1399**
Average resolution time [s/iter]		2.7456	2.718	2.7652	2.7479	2.7334	2.7668	2.8734

The bold represents the BCS of OF.

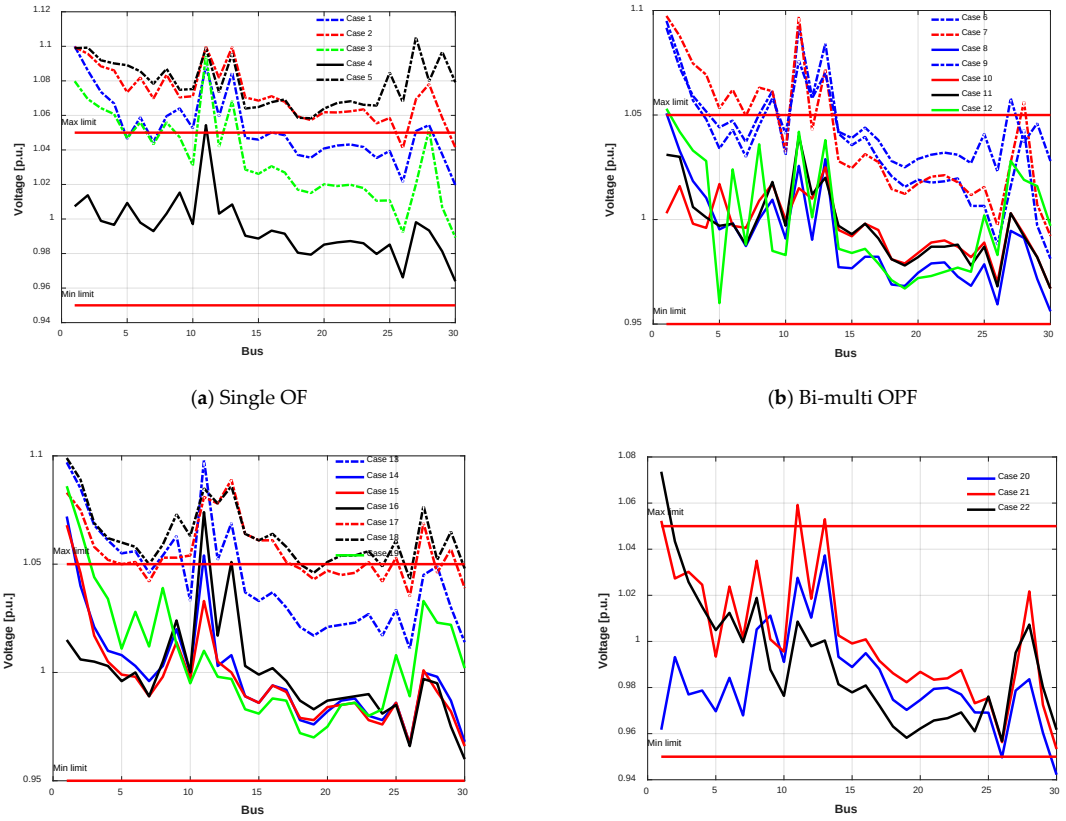

(**a**) Single OF

(**b**) Bi-multi OPF

(**c**) Tri-multi OPF

(**d**) Quad and Quinta multi OPF

Figure 9. The voltage profiles for cases 1 to case 22.

Figure 10a–f shows the values of the reactive power output from the generators for all cases (1–22). It can be observed that the MVAr of some generators (1, 5, and 8) exceeds the minimum and maximum limit in cases (1, 2, 5, 10, 12, 19, and 20). While the remaining generators have not violated the constraints in all cases.

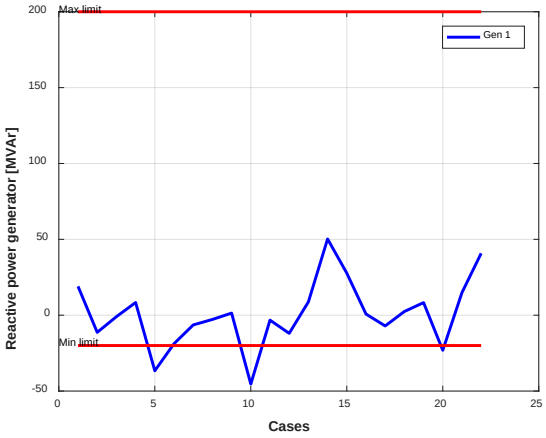

(**a**) Generator 1

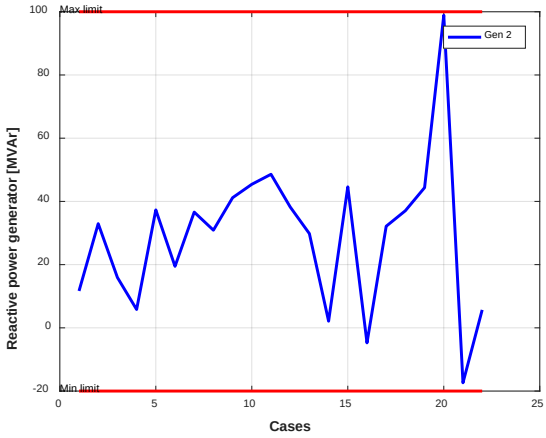

(**b**) Generator 2

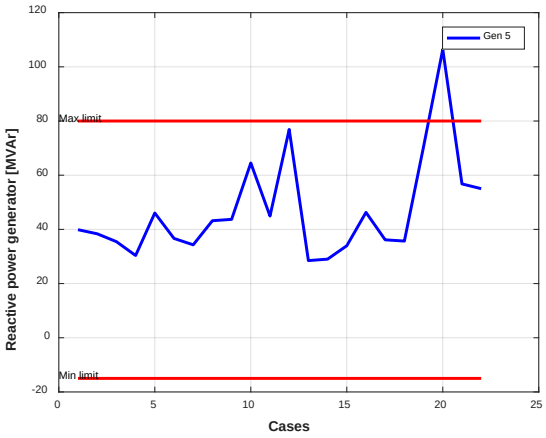

(**c**) Generator 5

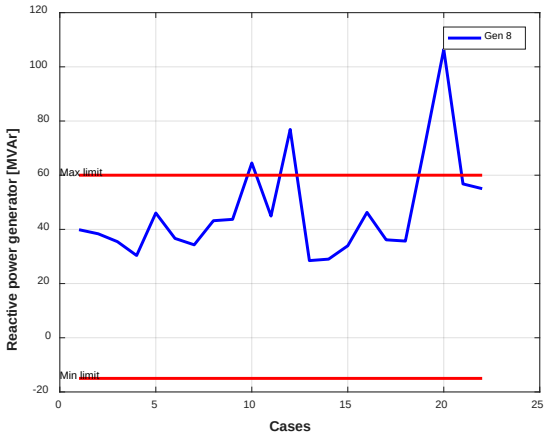

(**d**) Generator 8

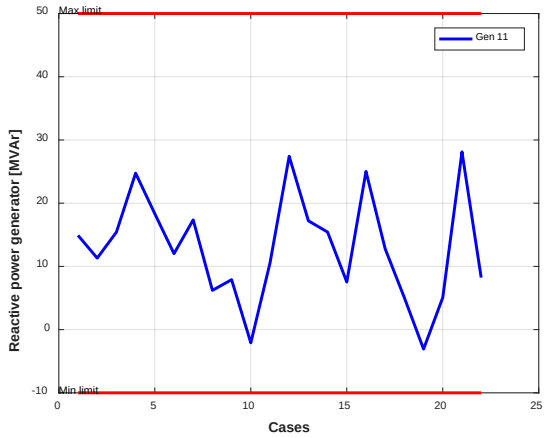

(**e**) Generator 11

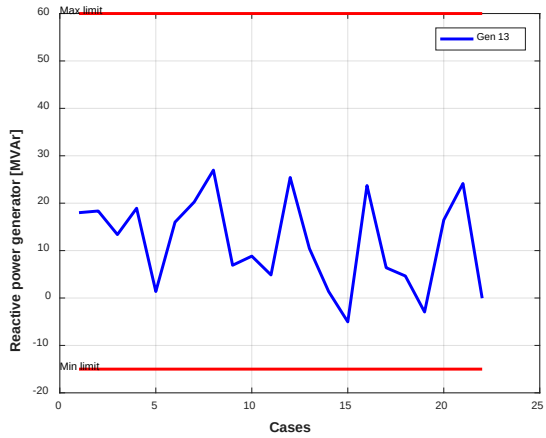

(**f**) Generator 13

Figure 10. Reactive power output from generators for cases (1−22).

4.2. IEEE 57-Bus Power System

The second test system applied in the paper to validate the effectiveness and superiority of the proposed algorithm HGS is the IEEE 57 bus power system, as shown in Figure 11. The control variables in the OPF problem for the IEEE 57-bus system are 33. The cost and emission coefficients of IEEE 57 bus power system are illustrated in Table 9. The optimal value control variables obtained by the proposed algorithm HGS are reported in Table 10.

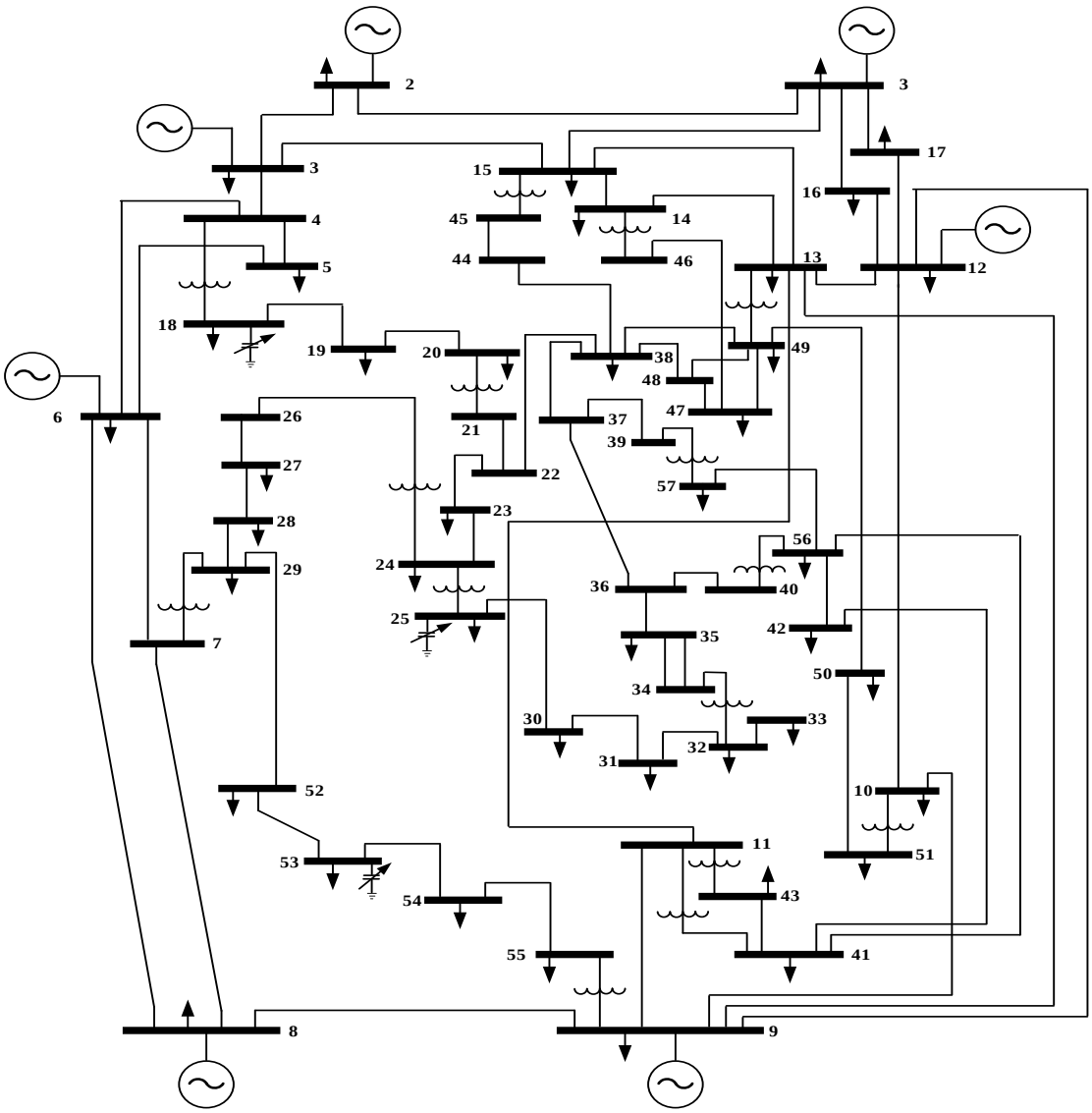

Figure 11. Single line diagram of the IEEE 57-bus system.

Single Objective OPF

The objective functions that are minimized are fuel cost [$/h], active power losses [MW], and emission [ton/h]. The parameters chosen in the proposed algorithm HGS to solve OPF problem are 100 iterations and 100 population sizes.

Case #23: Total fuel cost was minimized from 51,353 [$/h] (initial) to 41,679.4 [$/h] (the better), and the reduction rate was 18.84%, as illustrated in Table 10. The convergence plot of fuel cost [$/h] is depicted in Figure 12a.

Table 9. The cost and emission coefficients for generators for the IEEE 57-bus test system.

	Coefficient Generating Unit						
	G1	G2	G3	G6	G8	G9	G12
	Fuel cost coefficient						
a	0	0	0	0	0	0	0
b	2	1.75	3	2	1	1.75	3.25
c	0.00375	0.0175	0.025	0.00375	0.0625	0.0195	0.00834
	Emission coefficient						
α	4.091	2.543	6.131	3.491	4.258	2.754	5.326
β	−5.554	−6.047	−5.555	−5.754	−5.094	−5.847	−3.555
γ	6.49	5.638	5.151	6.39	4.586	5.238	3.38
ζ	2.0×10^{-4}	5.0×10^{-4}	1.0×10^{-5}	3.0×10^{-4}	1.0^{-6}	4.0×10^{-4}	2.0×10^{-3}
λ	2.857×10^{-1}	3.33×10^{-1}	6.67×10^{-1}	2.66×10^{-1}	8.0×10^{-1}	2.88×10^{-1}	2.0×10^{-1}

Table 10. Better control variables obtained by HGS for cases (23−25).

Item		**Limit**		**Initial**	**Case**		
		Max	**Min**		**#23**	**#24**	**#25**
[MW]	P_1	0.0	576	478	147.65	180.33	191.87
	P_2	30.0	100	0	92.19	28.74	99.34
	P_3	40.0	140	40	46.14	124.68	138.93
	P_6	30.0	100	0	68.59	33.74	99.88
	P_8	100.0	550	450	463.81	390.93	282.28
	P_9	30.0	100	0	84.31	94.41	99.84
	P_{12}	100.0	410	310	363.11	409.80	353.99
[p.u.]	V_1	0.95	1.10	1.040	1.07	1.07	1.02
	V_2	0.95	1.10	1.010	1.07	1.08	1.02
	V_3	0.95	1.10	0.985	1.06	1.07	1.02
	V_6	0.95	1.10	0.980	1.06	1.06	1.02
	V_8	0.95	1.10	1.005	1.09	1.08	1.04
	V_9	0.95	1.10	0.980	1.08	1.06	1.04
	V_{12}	0.95	1.10	1.015	1.06	1.05	1.01
Tap Position	T_{4-18}	0.90	1.10	0.97	1.02	1.02	1.01
	T_{4-18}	0.90	1.10	0.978	1.02	1.05	1.04
	T_{21-20}	0.90	1.10	1.043	0.98	0.99	1.01
	T_{24-25}	0.90	1.10	1	1.03	1.04	0.99
	T_{24-25}	0.90	1.10	1	1.04	1.03	0.99
	T_{24-26}	0.90	1.10	1.043	1.06	1.00	1.01
	T_{7-29}	0.90	1.10	0.967	1.05	1.05	0.99
	T_{34-32}	0.90	1.10	0.975	0.98	0.97	0.98
	T_{11-41}	0.90	1.10	0.955	1.02	1.09	1.03
	T_{15-45}	0.90	1.10	0.955	1.00	1.05	1.01
	T_{14-46}	0.90	1.10	0.9	1.01	1.05	1.00
	T_{10-51}	0.90	1.10	0.93	1.03	1.09	0.97
	T_{13-46}	0.90	1.10	0.895	0.95	1.02	1.00
	T_{11-43}	0.90	1.10	0.958	1.03	1.02	1.08
	T_{40-56}	0.90	1.10	0.958	1.00	0.98	1.05
	T_{39-57}	0.90	1.10	0.98	0.99	1.00	1.02
	T_{9-55}	0.90	1.10	0.94	1.06	1.03	1.02
[MVAr]	Q_{c18}	0.00	20	10	12.58	26.08	11.25
	Q_{25}	0.00	20	5.9	22.16	21.56	10.78
	Q_{53}	0.00	20	6.3	12.78	10.89	18.02

Table 10. *Cont.*

Item	Limit		Initial	Case		
	Max	Min		#23	#24	#25
GFC [$/h]			51353	**41679.4**	43740	45118
RPL [MW]			2.4129	15.24	**11.829**	15.6796
Em [ton/h]			27.868	1.3746	1.3048	**0.9616**
Reduction rate			-	18.84%	57.55%	60.15%
Average resolution time [s/iter]			-	12.257	12.225	12.24

The bold represents the better values of OF obtained by the proposed approach.

Case #24: Active power losses are minimized from 27.868 [MW] (initial) to 11.829 [MW] (the better); the reduction rate is 57.55%. The convergence speed of this case is illustrated in Figure 12b.

Case #25: Figure 12c illustrates the variations of emission over iteration. The better value of emission is 0.962 [ton/h]. The reduction rate is 60.15%.

The better control variables for the IEEE 57 bus system that are obtained by the HGS algorithm are depicted in Table 10. The bold represents the better values of OF obtained by the proposed approach.

Table 11 compares the numerical results obtained by HGS with other recent optimization methods for fuel cost [$/h], active power losses [MW], and emission [ton/h].

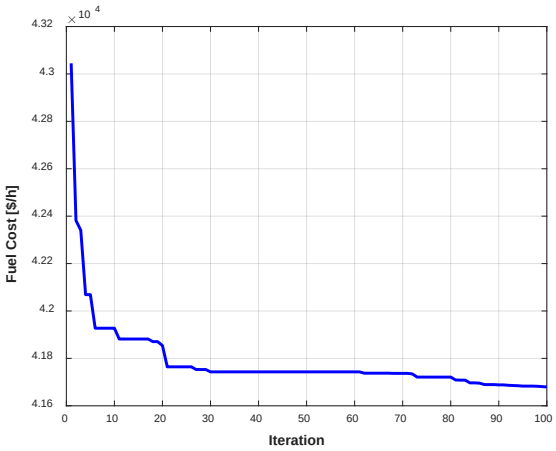

(**a**) Case #23

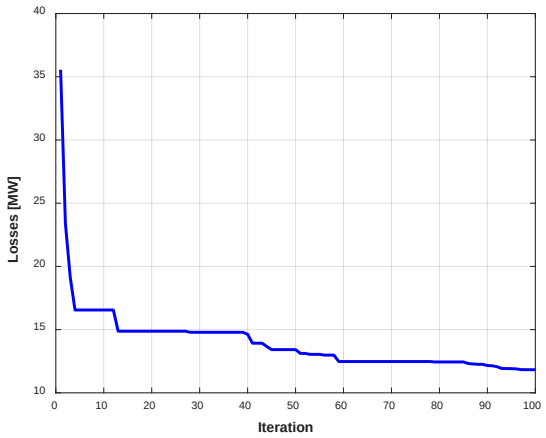

(**b**) Case #24

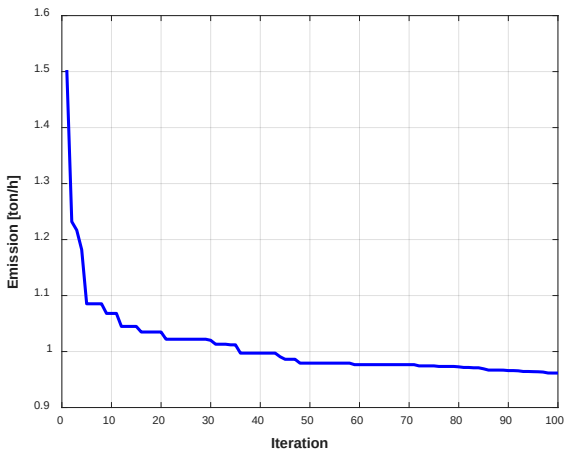

(**c**) Case #25

Figure 12. Convergence plot of HGS on the IEEE 57-bus system.

Table 11. Comparison of the numerical results obtained by HGS with other algorithms for cases (23−25).

Case #23		Case #24		Case #25	
Method	**FC [ton/h]**	**Method**	**RPL [p.u]**	**Method**	**Em [ton/h]**
GOA [37]	41680	ABC [41]	12.6260	ABC [41]	1.2048
GA [37]	41685	MICA [58]	11.8826	IABC [41]	1.0484
TLBO [37]	41683	GA [59]	13.3983	Jaya [59]	1.1111
MO-DEA [23]	41683	PSO [59]	13.6673	GA [59]	1.189
ABC [47]	41694	**HGS**	**11.83**	PSO [59]	1.19
GSA [60]	41695			MTLBO [61]	1.0772
NPSO [62]	41699.52			MICA [58]	1.2246
KHA [63]	41709.3			GBBICA [64]	1.1724
EADDE [65]	41713.6			SKHA [66]	1.08
fuzzy GA [67]	41716.3			SSO [28]	1.7024
HGS	**41679.4**			NISSO [28]	1.03927
				HGS	**0.9616**

The bold represents the better values of OF obtained by the proposed HGS approach.

The voltage profiles at each load bus for the IEEE 57 bus test system are charted in Figure 13. Voltage limits [0.94–1.06 p.u.] were exceeded on some buses. The exceeding of admissible voltage deviation at load buses may be attributed to several reasons. One of the most important reasons is the fact that we have a single objective function for these cases (23–25), and the voltage deviation was not considered an objective function for these cases. The reactive power of generators (2, 6, and 9) has violated the limits, while for the reactive power output for the generators (1, 3, 8, and 12), the constraints were not violated. The reactive power output for the generators in cases (23–25) is shown in Figure 14.

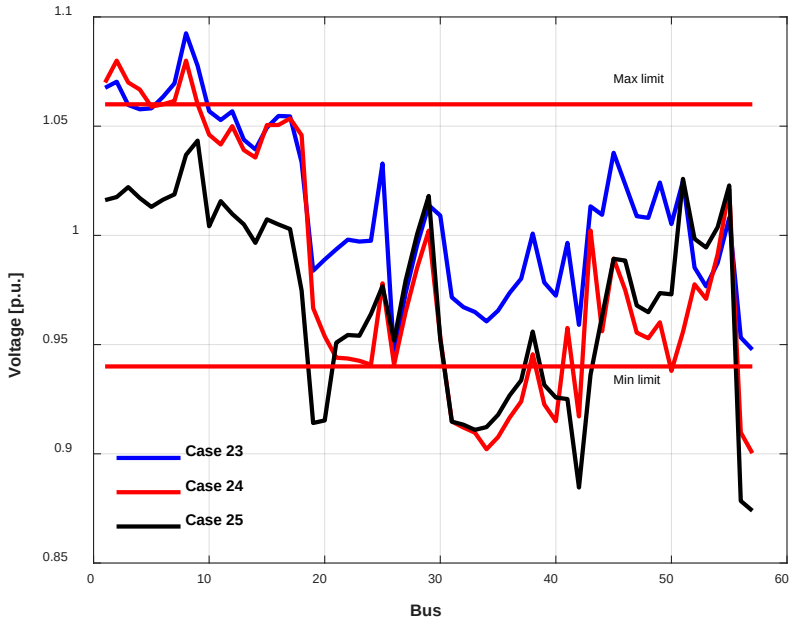

Figure 13. The voltage profiles for cases (23–25).

4.3. Discussions

To demonstrate the efficiency and the performance of the proposed HGS algorithm and of the developed MOHGS approach, the proposed approaches were applied in power systems to solve single and multiple OPF. For solving multi-objective optimal power flow (MOOPF) problems, the authors have developed the proposed HGS algorithm considering a new approach, namely, the multi-objective hunger game search (MOHGS), by merging with Pareto concept optimization to obtain a better distribution of non-dominated solutions

in the Pareto front set. In this article, the numerical results listed in Table 4 confirmed the ability of the proposed HGS algorithm to find good convergence and the better solution compared with state-of-the-art computational algorithms. Furthermore, the simulation results drawn in Figures 7 and 8 confirmed the very good capability of the developed MOHGS approach to achieve the convergence characteristics and the well-distribution in the Pareto front set.

The single and multi-objective OPF problems faced many challenges, the most important of which were the accurate convergence to reach the global optimal solution and uniform distribution of the Pareto front set (high coverage). In other words, a balance should be found between coverage and convergence. Based on the free lunch theorem (NFL) [68], can one heuristic meta algorithm solve all optimization problems? This reason, in addition to convergence and coverage, represents the main reasons concerning the non-superiority of some algorithms over others. The proposed approaches provide more diversification in the search space and highly boost exploitation by founding very good quality solutions and a very good distribution as well. Furthermore, the proposed MOHGS approach can solve more complex problems with less computational effort. Briefly, the obtained results by HGS and MOHGS can provide most convenient solutions of Pareto front set with good coverage and convergence along one, two, and three objectives when applied to solve OPF problems.

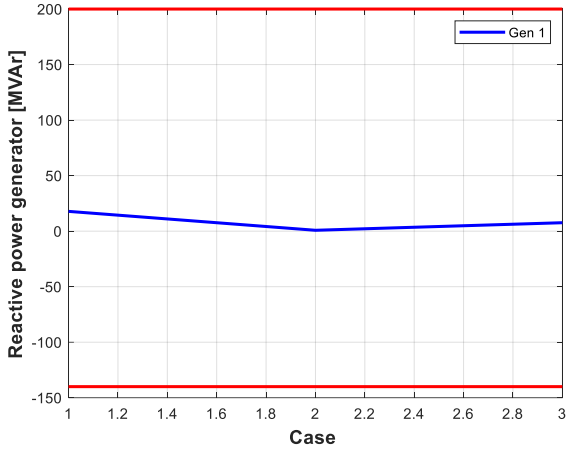

(**a**) Generator 1

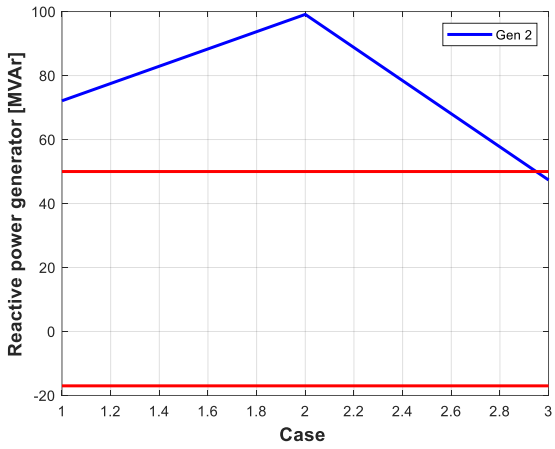

(**b**) Generator 2

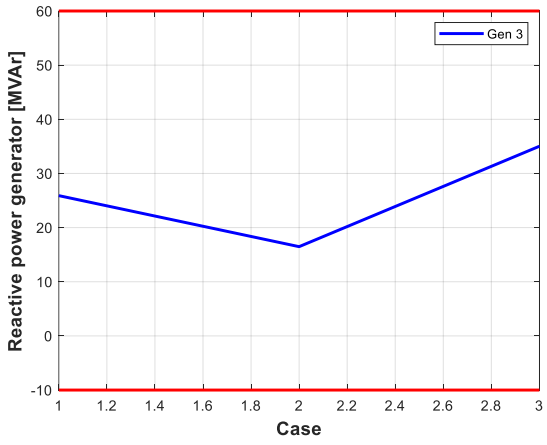

(**c**) Generator 3

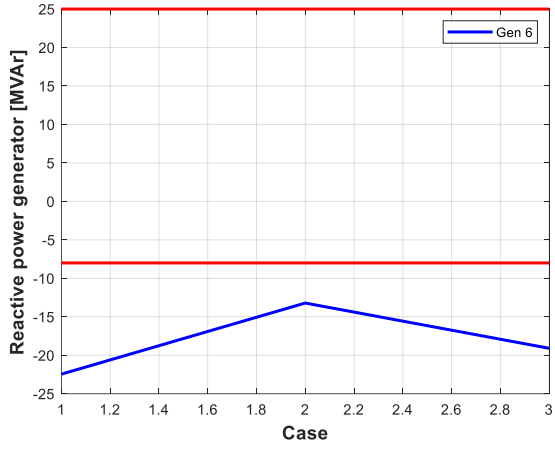

(**d**) Generator 6

Figure 14. *Cont.*

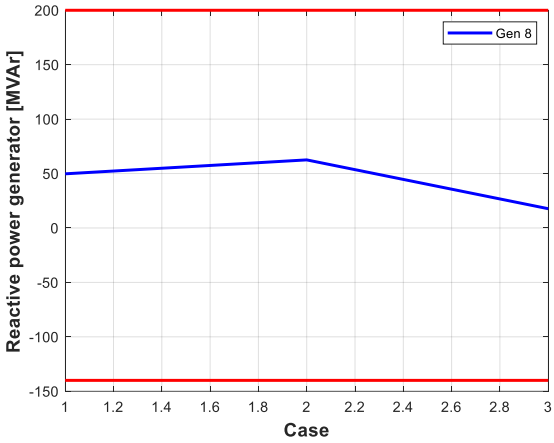

(**e**) Generator 8

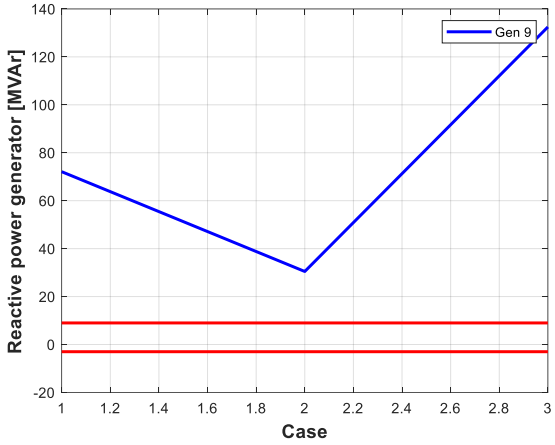

(**f**) Generator 9

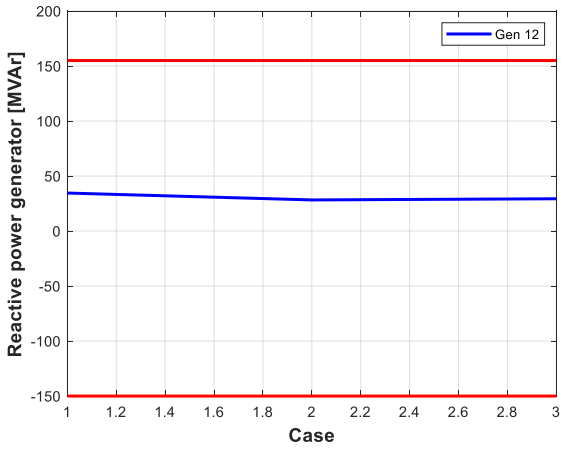

(**g**) Generator 12

Figure 14. Reactive power output for generators in cases (23−25).

5. Conclusions

In this study, a new optimization algorithm was tested, namely, the hunger games search (HGS), inspired by the behavior of social animal cooperation that is proportional to their level of hunger. This algorithm is proposed for solving the single objective optimal power flow problems in power systems to achieve the economical, technical, and environmental benefits. The HGS algorithm was developed to obtain better solutions for multiple conflicting objective functions simultaneously, namely, the multi-objective hunger games search (MOHGS). Various objective functions were considered, which are fuel cost [$/h], active power losses [MW], emission [ton/h], voltage deviation [p.u.], and voltage stability index. The optimization method that was used to determine the non-dominated solutions in the Pareto front set was the Pareto concept. The strategies that were used to extract BCS and rerank the non-dominated solutions were fuzzy set theory and crowding distance. To demonstrate the efficiency and capability of the proposed HGS algorithm and developed MOHGS approach, two power systems were used (IEEE 30-bus and IEEE 57-bus) for various single and multiple objective functions. The simulation results, illustrating the performance of the proposed approaches, are characterized by good convergence speed, well-distribution, and high efficiency. The comparison results with other well-known optimization methods confirmed the quality and robustness of the proposed approaches. Finally, the MOHGS is a reliable and robust optimization method to solve a multi-objective optimal power flow problem.

Author Contributions: Conceptualization, M.A.-K. and V.D.; methodology, M.A.-K.; software, M.A.-K.; validation, M.A.-K., V.D. and M.E.; formal analysis, M.A.-K.; investigation, M.A.-K. and V.D.; data curation, M.A.-K.; writing—original draft preparation, M.A.-K.; writing—review and editing, V.D. and M.E.; visualization, M.A.-K. and V.D.; supervision, V.D. and M.E.; project administration, M.E.; funding acquisition, V.D. All authors have read and agreed to the published version of the manuscript.

Funding: This research was funded by University POLITEHNICA of Bucharest.

Data Availability Statement: The data supporting the reported results are available in the manuscript.

Acknowledgments: This project was supported by the University POLITEHNICA of Bucharest in Romania, funded by the University POLITEHNICA of Bucharest.

Conflicts of Interest: The authors declare no conflict of interest.

References

1. Carpentier, J. Contribution to the economic dispatch problem. *Bull. Soc. Fr. Electr.* **1962**, *3*, 431–447.
2. Frank, S.; Steponavice, I.; Rebennack, S. Optimal power flow: A bibliographic survey I. *Energy Syst.* **2012**, *3*, 221–258. [CrossRef]
3. Al-Bahrani, L.; Al-kaabi, M.; Al-saadi, M.; Dumbrava, V. Optimal power flow based on differential evolution optimization technique. *U.P.B. Sci. Bull. Ser. C* **2020**, *82*, 378–388.
4. Bouktir, T.; Slimani, L.; Belkacemi, M. A genetic algorithm for solving the optimal power flow problem. *Leonardo J. Sci.* **2004**, *4*, 44–58.
5. Al-kaabi, M.; Al-Bahrani, L. Modified Artificial Bee Colony Optimization Technique with Different Objective Function of Constraints Optimal Power Flow. *Int. J. Intell. Eng. Syst.* **2020**, *13*, 378–388. [CrossRef]
6. Al-Kaabi, M.; Al-Bahrani, L.; Dumbrava, V.; Eremia, M. Optimal Power Flow with Four Objective Functions using Improved Differential Evolution Algorithm: Case Study IEEE 57-bus power system. In Proceedings of the 2021 10th International Conference Energy and Environment, Bucharest, Romania, 14–15 October 2021; pp. 1–5. [CrossRef]
7. Al-Bahrani, L.; Al-Kaabi, M.; Al-Hasheme, J. Solving Optimal Power Flow Problem Using Improved Differential Evolution Algorithm. *Int. J. Electr. Electron. Eng. Telecommun.* **2022**, *11*, 146–155. [CrossRef]
8. Li, S.; Gong, W.; Hu, C.; Yan, X.; Wang, L.; Gu, Q. Adaptive constraint differential evolution for optimal power flow. *Energy* **2021**, *235*, 12136. [CrossRef]
9. Li, S.; Gong, W.; Wang, L.; Yan, X.; Hu, C. Optimal power flow by means of improved adaptive differential evolution. *Energy* **2020**, *198*, 117314. [CrossRef]
10. Meng, A.; Zeng, C.; Wang, P.; Chen, D.; Zhou, T.; Zheng, X.; Yin, H. A high-performance crisscross search based grey wolf optimizer for solving optimal power flow problem. *Energy* **2021**, *225*, 120211. [CrossRef]
11. Al-Kaabi, M.; Al Hasheme, J.; Dumbrava, V.; Eremia, M. Application of Harris Hawks Optimization (HHO) Based on Five Single Objective Optimal Power Flow. In Proceedings of the 2022 14th International Conference on Electronics, Computers and Artificial Intelligence (ECAI), Ploesti, Romania, 30 June–1 July 2022; pp. 1–8. [CrossRef]
12. Arsyad, H.; Suyuti, A.; Said, S.M.; Akil, Y.S. Multi-objective dynamic economic dispatch using Fruit Fly Optimization method. *Arch. Electr. Eng.* **2021**, *70*, 351–366. [CrossRef]
13. Al-Kaabi, M.; Al-Bahrani, L.; Al Hasheme, J. Improved Differential Evolution Algorithm to solve multi-objective of optimal power flow problem. *Arch. Electr. Eng.* **2022**, *71*, 641–657. [CrossRef]
14. Al-Kaabi, M.; Dumbrava, V.; Eremia, M. A Slime Mould Algorithm Programming for Solving Single and Multi-Objective Optimal Power Flow Problems with Pareto Front Approach: A Case Study of the Iraqi Super Grid High Voltage. *Energies* **2022**, *15*, 7473. [CrossRef]
15. Daqaq, F.; Ouassaid, M.; Ellaia, R. A new meta-heuristic programming for multi-objective optimal power flow. *Electr. Eng.* **2021**, *103*, 1217–1237. [CrossRef]
16. Avvari, R.K.; Vinod Kumar, D.M. Multi-Objective Optimal Power Flow with efficient Constraint Handling using Hybrid Decomposition and Local Dominance Method. *J. Inst. Eng. Ser. B* **2022**, *103*, 1643–1658. [CrossRef]
17. Huy, T.H.B.; Kim, D.; Vo, D.N. Multiobjective Optimal Power Flow Using Multiobjective Search Group Algorithm. *IEEE Access* **2022**, *10*, 77837–77856. [CrossRef]
18. Yang, Y.; Chen, H.; Heidari, A.A.; Gandomi, A.H. Hunger games search: Visions, conception, implementation, deep analysis, perspectives, and towards performance shifts. *Expert Syst. Appl.* **2021**, *177*, 114864. [CrossRef]
19. Khunkitti, S.; Siritaratiwat, A.; Premrudeepreechacharn, S. Multi-Objective optimal power flow problems based on Slime mould algorithm. *Sustainability* **2021**, *13*, 7448. [CrossRef]
20. Premkumar, M.; Jangir, P.; Sowmya, R.; Elavarasan, R.M. Many-Objective Gradient-Based Optimizer to Solve Optimal Power Flow Problems: Analysis and Validations. *Eng. Appl. Artif. Intell.* **2021**, *106*, 104479. [CrossRef]
21. Barocio, E.; Regalado, J.; Cuevas, E.; Uribe, F.; Zúñiga, P.; Torres, P.J.R. Modified bio-inspired optimisation algorithm with a centroid decision making approach for solving a multi-objective optimal power flow problem. *IET Gener. Transm. Distrib.* **2017**, *11*, 1012–1022. [CrossRef]

22. Niknam, T.; rasoul Narimani, M.; Jabbari, M.; Malekpour, A.R. A modified shuffle frog leaping algorithm for multi-objective optimal power flow. *Energy* **2011**, *36*, 6420–6432. [CrossRef]
23. Shaheen, A.M.; El-Sehiemy, R.A.; Farrag, S.M. Solving multi-objective optimal power flow problem via forced initialised differential evolution algorithm. *IET Gener. Transm. Distrib.* **2016**, *10*, 1634–1647. [CrossRef]
24. Sivasubramani, S.; Swarup, K.S. Multi-objective harmony search algorithm for optimal power flow problem. *Int. J. Electr. Power Energy Syst.* **2011**, *33*, 745–752. [CrossRef]
25. Varadarajan, M.; Swarup, K.S. Solving multi-objective optimal power flow using differential evolution. *IET Gener. Transm. Distrib.* **2008**, *2*, 720–730. [CrossRef]
26. Bouchekara, H. Optimal power flow using black-hole-based optimization approach. *Appl. Soft Comput.* **2014**, *24*, 879–888. [CrossRef]
27. Attia, A.; El Sehiemy, R.; Hasanien, H. Optimal power flow solution in power systems using a novel Sine-Cosine algorithm. *Int. J. Electr. Power Energy Syst.* **2018**, *99*, 331–343. [CrossRef]
28. Nguyen, T. A high performance social spider optimization algorithm for optimal power flow solution with single objective optimization. *Energy* **2019**, *171*, 218–240. [CrossRef]
29. Abaci, K.; Yamacli, V. Differential search algorithm for solving multi-objective optimal power flow problem. *Int. J. Electr. Power Energy Syst.* **2016**, *79*, 1–10. [CrossRef]
30. El-Hana Bouchekara, H.R.; Abido, M.A.; Chaib, A.E. Optimal power flow using an improved electromagnetism-like mechanism method. *Electr. Power Compon. Syst.* **2016**, *44*, 434–449. [CrossRef]
31. Warid, W.; Hizam, H.; Mariun, N.; Abdul-Wahab, N.I. Optimal power flow using the Jaya algorithm. *Energies* **2016**, *9*, 678. [CrossRef]
32. Roberge, V.; Tarbouchi, M.; Okou, F. Optimal power flow based on parallel metaheuristics for graphics processing units. *Electr. Power Syst. Res.* **2016**, *140*, 344–353. [CrossRef]
33. Mohamed, A.; Mohamed, Y.S.; El-Gaafary, A.A.M.; Hemeida, A.M. Optimal power flow using moth swarm algorithm. *Electr. Power Syst. Res.* **2017**, *142*, 190–206. [CrossRef]
34. Kumari, M.S.; Maheswarapu, S. Enhanced genetic algorithm based computation technique for multi-objective optimal power flow solution. *Int. J. Electr. Power Energy Syst.* **2010**, *32*, 736–742. [CrossRef]
35. Biswas, P.P.; Suganthan, P.N.; Mallipeddi, R.; Amaratunga, G.A.J. Optimal power flow solutions using differential evolution algorithm integrated with effective constraint handling techniques. *Eng. Appl. Artif. Intell.* **2018**, *68*, 81–100. [CrossRef]
36. Abdel-Rahim, A.M.; Shaaban, S.A.; Raglend, I.J. Optimal Power Flow Using Atom Search Optimization. In Proceedings of the 2019 Innovations in Power and Advanced Computing Technologies (i-PACT), Vellore, India, 22–23 March 2019; pp. 1–4. [CrossRef]
37. Taher, M.A.; Kamel, S.; Jurado, F.; Ebeed, M. Modified grasshopper optimization framework for optimal power flow solution. *Electr. Eng.* **2019**, *101*, 121–148. [CrossRef]
38. Surender Reddy, B.P. Efficiency improvements in meta-heuristic algorithms to solve the optimal power flow problem. *Int. J. Electr. Power Energy Syst.* **2016**, *82*, 288–302. [CrossRef]
39. Warid, W. Optimal power flow using the AMTPG-Jaya algorithm. *Appl. Soft Comput.* **2020**, *91*, 106252. [CrossRef]
40. Naderi, E.; Pourakbari-Kasmaei, M.; Cerna, F.V.; Lehtonen, M. A novel hybrid self-adaptive heuristic algorithm to handle single-and multi-objective optimal power flow problems. *Int. J. Electr. Power Energy Syst.* **2021**, *125*, 106492. [CrossRef]
41. He, X.; Wang, W.; Jiang, J.; Xu, L. An improved artificial bee colony algorithm and its application to multi-objective optimal power flow. *Energies* **2015**, *8*, 2412–2437. [CrossRef]
42. Niknam, T.; Narimani, M.R.; Aghaei, J.; Azizipanah-Abarghooee, R. Improved particle swarm optimisation for multi-objective optimal power flow considering the cost, loss, emission and voltage stability index. *IET Gener. Transm. Distrib.* **2012**, *6*, 515–527. [CrossRef]
43. Islam, M.Z.; Wahab, N.I.A.; Veerasamy, V.; Hizam, H.; Mailah, N.F.; Guerrero, J.M.; Mohd Nasir, M.N. A Harris Hawks Optimization Based Single-and Multi-Objective Optimal Power Flow Considering Environmental Emission. *Sustainability* **2020**, *12*, 5248. [CrossRef]
44. Bakirtzis, A.G.; Biskas, P.N.; Zoumas, C.E.; Petridis, V. Optimal power flow by enhanced genetic algorithm. *IEEE Trans. Power Syst.* **2002**, *17*, 229–236. [CrossRef]
45. Lai, L.L.; Ma, J.T.; Yokoyama, R.; Zhao, M. Improved genetic algorithms for optimal power flow under both normal and contingent operation states. *Int. J. Electr. Power Energy Syst.* **1997**, *19*, 287–292. [CrossRef]
46. Attia, A.; Al-Turki, Y.A.; Abusorrah, A.M. Optimal power flow using adapted genetic algorithm with adjusting population size. *Electr. Power Compon. Syst.* **2012**, *40*, 1285–1299. [CrossRef]
47. Adaryani, M.R.; Karami, A. Artificial bee colony algorithm for solving multi-objective optimal power flow problem. *Int. J. Electr. Power Energy Syst.* **2013**, *53*, 219–230. [CrossRef]
48. Radosavljević, J.; Klimenta, D.; Jevtić, M.; Arsić, N. Optimal Power Flow Using a Hybrid Optimization Algorithm of Particle Swarm Optimization and Gravitational Search Algorithm. *Electr. Power Compon. Syst.* **2015**, *43*, 1958–1970. [CrossRef]
49. Abd El-sattar, S.; Kamel, S.; Ebeed, M.; Jurado, F. An improved version of salp swarm algorithm for solving optimal power flow problem. *Soft Comput.* **2021**, *25*, 4027–4052. [CrossRef]

50. Duman, S. Symbiotic organisms search algorithm for optimal power flow problem based on valve-point effect and prohibited zones. *Neural Comput. Appl.* **2017**, *28*, 3571–3585. [CrossRef]
51. Chaib, A.E.; Bouchekara, H.; Mehasni, R.; Abido, M.A. Optimal power flow with emission and non-smooth cost functions using backtracking search optimization algorithm. *Int. J. Electr. Power Energy Syst.* **2016**, *81*, 64–77. [CrossRef]
52. Khan, A.; Hizam, H.; bin Abdul Wahab, N.I.; Lutfi Othman, M. Optimal power flow using hybrid firefly and particle swarm optimization algorithm. *PLoS ONE* **2020**, *15*, e0235668. [CrossRef]
53. Khorsandi, A.; Hosseinian, S.H.; Ghazanfari, A. Modified artificial bee colony algorithm based on fuzzy multi-objective technique for optimal power flow problem. *Electr. Power Syst. Res.* **2013**, *95*, 206–213. [CrossRef]
54. Kumar, A.R.; Premalatha, L. Optimal power flow for a deregulated power system using adaptive real coded biogeography-based optimization. *Int. J. Electr. Power Energy Syst.* **2015**, *73*, 393–399. [CrossRef]
55. Bouchekara, H.; Abido, M.A.; Boucherma, M. Optimal power flow using teaching-learning-based optimization technique. *Electr. Power Syst. Res.* **2014**, *114*, 49–59. [CrossRef]
56. Abido, M.A. Multiobjective optimal power flow using strength Pareto evolutionary algorithm. In Proceedings of the 39th International Universities Power Engineering Conference, Bristol, UK, 6–8 September 2004; pp. 457–461.
57. Abido, M.A.; Al-Ali, N.A. Multi-objective differential evolution for optimal power flow. In Proceedings of the 2009 International Conference on Power Engineering, Energy and Electrical Drives, Lisbon, Portugal, 18–20 March 2009; pp. 101–106. [CrossRef]
58. Ghasemi, M.; Ghavidel, S.; Ghanbarian, M.M.; Gharibzadeh, M.; Vahed, A.A. Multi-objective optimal power flow considering the cost, emission, voltage deviation and power losses using multi-objective modified imperialist competitive algorithm. *Energy* **2014**, *78*, 276–289. [CrossRef]
59. Abd El-Sattar, S.; Kamel, S.; El Sehiemy, R.A.; Jurado, F.; Yu, J. Single-and multi-objective optimal power flow frameworks using Jaya optimization technique. *Neural Comput. Appl.* **2019**, *31*, 8787–8806. [CrossRef]
60. Duman, S.; Güvenç, U.; Sönmez, Y.; Yörükeren, N. Optimal power flow using gravitational search algorithm. *Energy Convers. Manag.* **2012**, *59*, 86–95. [CrossRef]
61. Shabanpour-Haghighi, A.; Seifi, A.R.; Niknam, T. A modified teaching–learning based optimization for multi-objective optimal power flow problem. *Energy Convers. Manag.* **2014**, *77*, 597–607. [CrossRef]
62. Selvakumar, A.I.; Thanushkodi, K. A new particle swarm optimization solution to nonconvex economic dispatch problems. *IEEE Trans. Power Syst.* **2007**, *22*, 42–51. [CrossRef]
63. Roy, P.K.; Paul, C. Optimal power flow using krill herd algorithm. *Int. Trans. Electr. Energy Syst.* **2015**, *25*, 1397–1419. [CrossRef]
64. Ghasemi, M.; Ghavidel, S.; Ghanbarian, M.M.; Gitizadeh, M. Multi-objective optimal electric power planning in the power system using Gaussian bare-bones imperialist competitive algorithm. *Inf. Sci.* **2015**, *294*, 286–304. [CrossRef]
65. Vaisakh, K.; Srinivas, L.R. Evolving ant direction differential evolution for OPF with non-smooth cost functions. *Eng. Appl. Artif. Intell.* **2011**, *24*, 426–436. [CrossRef]
66. Pulluri, H.; Naresh, R.; Sharma, V. A solution network based on stud krill herd algorithm for optimal power flow problems. *Soft Comput.* **2018**, *22*, 159–176. [CrossRef]
67. Hsiao, Y.; Chen, C.; Chien, C. Optimal capacitor placement in distribution systems using a combination fuzzy-GA method. *Int. J. Electr. Power Energy Syst.* **2004**, *26*, 501–508. [CrossRef]
68. Wolpert, D.H.; Macready, W.G. *No Free Lunch Theorems for Search*; Technical Report SFI-TR-95-02-010; Santa Fe Institute: Santa Fe, NM, USA, 1995.